s-trans-1,3-Butadiene and Isotopomers: Vibrational Spectra, Scaled Quantum-Chemical Force Fields, Fermi Resonances, and C−H Bond Properties

Donald C. McKean,*,† Norman C. Craig,‡ and Yurii N. Panchenko§

School of Chemistry, University of Edinburgh, West Mains Road, Edinburgh EH9 3JJ, U.K., Department of Chemistry and Biochemistry, Oberlin College, Oberlin, Ohio 44074, and Laboratory of Molecular Spectroscopy, Division of Physical Chemistry, Department of Chemistry, M. V. Lomonosov Moscow State University, Moscow 119899, Russian Federation

Received: January 26, 2006; In Final Form: April 28, 2006

Quadratic quantum-chemical force fields have been determined for *s-trans*-1,3-butadiene using B3LYP and MP2 methods. Basis sets included 6-311++G**, cc-pVTZ, and aug-cc-pVTZ. Scaling of the force fields was based on frequency data for up to 11 isotopomers, some of these data being original. A total of 18 scale factors were employed, with, in addition, an alteration to one off-diagonal force constant in the A_u species. MP2 calculations without *f* functions in the basis perform badly in respect of out-of-plane bending mode frequencies. Centrifugal distortion constants and harmonic contributions to vibration−rotation constants (alphas) have been calculated. Existing experimental frequency data for all isotopomers are scrutinized, and a number of reassignments and diagnoses of Fermi resonance made, particularly in the ν(CH) region. The three types of CH bond in butadiene were characterized in terms of bond length and isolated CH stretching frequency, the latter reflecting data in the ν(CD) region. Broad agreement was achieved with earlier results from local mode studies. Differences in CH bond properties resemble similar differences in propene. A simplified sample setup for recording FT-Raman spectra of gases was applied to four isotopomers of butadiene.

Introduction

The molecule of *s-trans*-1,3-butadiene (BDE) forms the prototype of conjugated C═C systems and as such merits thorough investigations of both structure and vibrational properties. The absence of a permanent dipole moment in BDE has meant that experimental information concerning its structure has been limited to electron diffraction studies in the gas,[1] apart from a single microwave study of a partially deuterated isotopomer.[2] However, recent work on high-resolution infrared spectra of various isotopomers has provided enough ground state inertial parameters for spectroscopically based structures to be determined.[3−6] This work offers the further prospect of determining the first experimentally based equilibrium structure, provided the necessary harmonic and anharmonic adjustments ("alphas") to the ground state inertial constants can be obtained. For a number of molecules quantum-chemical (QC) calculations have been invoked to supply these alphas.[7−10] For all but the lightest molecules, scaling of the QC force constants for vibrational frequencies is considered necessary or advisable before applying them to the calculation of alphas. In one such procedure, applied by Groner,[8] the harmonic contributions to alphas are obtained from a QC quadratic force field scaled with a single factor while the anharmonic ones are derived from unscaled QC calculations of the cubic force constants. This technique has been used recently, with success, on the *cis*- and *trans*-1,2-difluoroethylenes[11] and, less profitably perhaps, on *cis*,*trans*-1,4 difluorobutadiene.[11]

Whereas this report focuses on the development of improved frequency assignments and force constants, a companion report will discuss the equilibrium structure and its implications for the understanding of double bond conjugation.[12] The prime object of the present work was therefore to provide the alphas needed for this route to an equilibrium geometry for BDE. However, other considerations suggested that the determination of a new scaled QC force field was timely.

First, a range of new frequency data for various isotopomers has been obtained in one of our laboratories, in addition to those[3−6] referenced above. This work adds to an abundance of data that already exists for a range of such isotopomers, whose sources will be reviewed as needed below. Together, these results improve the quality of the data available for the scaling procedure. Second, among a field of 12 different scaling approaches, summarized and characterized in the most recent of these scaling studies on BDE,[13] little or no attempt has been made to identify inconsistencies in the experimental data, especially those arising from Fermi resonance. A quality scaled QC force field can throw useful light on the presence and magnitude of such resonances. It can also help to identify possible misassignments of vibration frequencies, which in our experience can persist undetected in the literature over the decades.[14]

The regions of the spectrum where such resonances are most prevalent in organic compounds are those involving the stretching of CH and CD bonds. Potentially, these regions are the source of vital information about the relative strengths of individual CH bonds.[15] In every one of the numerous QC calculations of the geometry of BDE, the three types of CH bond, which are conveniently designated CH_t, CH_c, and CH_α according to their relation as trans, cis, or α to the second vinyl group (Figure 1), are found to differ in their lengths in a consistent way, with $r(C-H_\alpha) > r(C-H_c) > r(C-H_t)$.[13,16] Such differences can be linked with great precision to variations in

† School of Chemistry, University of Edinburgh.
‡ Department of Chemistry and Biochemistry, Oberlin College.
§ Department of Chemistry, M. V. Lomonosov Moscow State University.

10.1021/jp060566v CCC: $33.50
Published on Web 06/15/2006

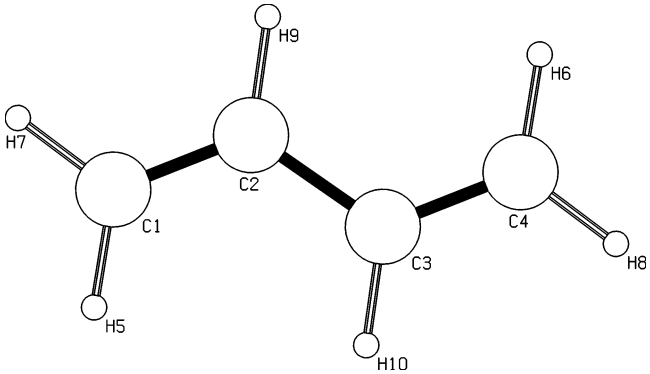

Figure 1. Structure and atom numbering for the *s-trans*-1,3-butadiene model. H_5, $H_6 = H_c$; H_7, $H_8 = H_t$; H_9, $H_{10} = H_\alpha$.

the so-called isolated stretching frequencies, ν^{is}(CH), in which all CH bonds in the molecule bar one are substituted by deuterium.[15,17−19]

Detailed studies in the overtone regions of both undeuterated and partially deuterated (d_5) species have already identified differing local mode frequencies for these three types of CH bond in the order expected from their relative bond lengths.[20] It remains to be seen if the fundamental regions of the various isotopomers can be explained in the same way, with a satisfactory interpretation of the Fermi resonances which are prevalent here. These are expected to involve primarily combination levels resulting from δ(CH) and ν(C═C) quanta, but other levels such as 2ν(C═C) may be involved.[21]

Such an investigation proved successful in a recent study of *cis*- and *trans*-1,2-difluoroethylenes.[14] However, with the presence of three types of CH bond and two sets of δ(CH) and ν(C═C) frequencies, BDE represents a much harder problem.

Experimental Section

With the exception of a few bands that were investigated with high-resolution infrared spectroscopy, extended and revised assignments for frequencies of vibrational fundamentals of BDE and a number of its isotopomers came from medium-resolution spectroscopy. The mid-infrared spectra were recorded for gas-phase samples on a Nicolet 760 Magna spectrometer with a resolution of approximately 0.08 cm^{-1} unapodized. The far-infrared spectra were recorded on a Perkin-Elmer 1700X spectrometer with 1 cm^{-1} resolution. Where infrared frequencies are reported to more than one decimal place, the rotational structure in the band has been analyzed.[3−6]

Raman spectra were obtained with a Raman module associated with the 760 spectrometer. Excitation was with a Nd:YVO_4 laser at 1064 nm, and detection was with a germanium device cooled with liquid nitrogen. The 90° optical system with an associated polarization analyzer was used for the liquid-phase spectra. Samples were sealed in 1.8 mm (o.d.) capillaries and studied as liquids at room temperature. Laser power was typically about 0.5 W, resolution was 2 cm^{-1}, and about 4000 scans were accumulated for each setting of the polarization analyzer. For gas-phase Raman spectra, an exceptionally simple sample arrangement was employed. Samples were sealed in standard-wall 5 mm (o.d.) NMR tubes and examined with the more efficient 180° optical system. The sample holder was a vertical, gold-plated half cylinder. The laser power was about 1.6 W, the resolution was 4 cm^{-1}, and 8000 scans (Ge detector) or 16 000 scans (InGaAs detector) were accumulated. Caused by laser heating, the temperature rose to about 40 °C in the sample compartment. At this temperature, the vapor pressure of butadiene above the small pool of liquid is about 4 atm.

The isotopomers studied in the Raman effect were those commercially available, namely the normal, 2,3-d_2, 1,1,4,4-d_4, and d_6 species, respectively. The gas-phase frequencies obtained agreed within 1−2 cm^{-1} with those obtained previously by Wiberg and Rosenberg.[22]

Because the only reported source of the actual gas-phase Raman spectra of these four species is relatively inaccessible in Rosenberg's Ph.D. thesis,[23] our gas-phase Raman spectra are supplied in the Supporting Information in Figures S1−S4. As far as is possible, new observations of fundamental frequencies are used in the tables in this paper. In most cases, the adjustments are small, and some supersede our earlier publications. However, earlier observations of some modes are included, as are some reassignments and the resolution of Fermi resonances. New data of significance are designated in the above tables in boldface type.

Theoretical Section

MP2 and B3LYP calculations were performed using the Gaussian programs G98 or G03.[24] The complete force field was studied using one of two types of basis set; the Pople type 6-311++G** and the Dunning correlation-consistent cc-pVTZ.[25,26] A single B3LYP force field calculation was also carried out with the Dunning aug-cc-pVTZ basis set, which includes diffuse functions.[26] In addition, the A_u/B_g vibrational force field was also studied with the 6-31G* and 6-311G** bases. For convenience in the tables below, the following abbreviations are used: B3LYP/6-31G* ("dsv"), B3LYP/6-311G** ("dtz"), B3LYP/6-311++G** ("dtz+"), B3LYP/cc-pVTZ ("dcct"), B3LYP/aug-cc-pVTZ)("dcct+"), MP2/6-31G* ("msv"), MP2/6-311G** ("mtz"), MP2/6-311++G** ("mtz+"), and MP2/cc-pVTZ ("mcct"). Convergence in the prior geometry optimizations was controlled by the "tight" option. For the density functional calculations a grid of 99 shells, each containing 302 points, was employed, as in previous work from our laboratories.[14]

Repetition of a given calculation from differing starting geometries gave frequencies agreeing within 0.05 cm^{-1}. Bond lengths were similarly reproduced to within about 0.00002 Å. This reproducibility is relevant to our interest in the small differences in properties exhibited by the three types of CH bond. Table 1 shows the equilibrium geometries obtained in this work, on the basis of which the subsequent force fields were calculated. The calculated bond length differences $\Delta r(CH_c-CH_t)$ of 0.0021−0.0023 Å and $\Delta r(CH_\alpha-CH_c)$ of 0.0026−0.0030 Å are highly consistent with each other and well reproduced in the semiexperimental equilibrium structure.

Calculations were performed either on a DEC Alpha 1000 workstation or using the resources of the EPSRC National Service for Computational Chemistry Software, on Columbus, a cluster of 6 HP ES40 computers, each of which has four 833 MHz EV68 CPUs and 8 GB of memory.

For the calculation of force constants on a symmetry coordinate basis and subsequent scaling, the Gaussian output of Cartesian-based force constants was input into the program ASYM40.[27] The scaling procedure requires a detailed, separate discussion.

Analysis of Data and Discussion

Procedures for the Scaling of the QC Force Field. BDE has exemplified the whole range of approaches that may be made to the scaling of a QC quadratic force field. These vary primarily according to the objective of each exercise. For the prediction of the frequencies of one molecule from data obtained

TABLE 1: Comparison of QC and Experimental Equilibrium Geometric Parameters for *trans*-1,3-Butadiene

	B3LYP[b]			MP2[b]		experiment	
parameter[a]	dtz+	dcct	dcct+	mtz+	mcct	E.D.[c]	IR/QC[d]
$r(C-H_\alpha)$	1.088 23	1.085 90	1.085 78	1.089 45	1.084 48	1.107	1.0847(10)
$r(C-H_t)$	1.083 33	1.080 92	1.080 82	1.084 75	1.079 71	1.107	1.0793(10)
$r(C-H_c)$	1.085 60	1.083 22	1.083 14	1.086 87	1.081 86	1.107	1.0819(10)
$\Delta r(C-H)_{c-t}$	0.0023	0.0023	0.0023	0.0021	0.0022		0.0026
$\Delta r(C-H)_{\alpha-c}$	0.0026	0.0027	0.0026	0.0030	0.0026		0.0028
$r(C=C)$	1.3384	1.3339	1.3344	1.3471	1.3401	1.348	1.3379(10)
$r(C_2-C_3)$	1.4562	1.4527	1.4527	1.4602	1.4533	1.468	1.4539(10)
$\angle(C_1C_2C_3)$	124.33	124.36	124.35	123.58	123.54	124.3	123.62(10)
$\angle(H_tCC)$	121.66	121.68	121.64	121.44	121.47	120.7	121.47(10)
$\angle(H_cCC)$	121.46	121.43	121.44	121.02	120.84	120.7	120.97(10)
$\angle(H_cCH_c)$	116.88	116.89	116.92	117.54	117.70		
$\angle(H_\alpha C_2C_1)$	119.33	119.34	119.32	119.57	119.60	120.7	119.9(1)
$\angle(H_\alpha C_2C_3)$	116.34	116.30	116.33	116.85	116.86		

[a] Bond lengths in angstroms; angles in degrees. [b] tz+ = 6-311++G**, cct = cc-pVTZ, and cct+ = aug-cc-pVTZ. [c] Reference 1. [d] Equilibrium structure found from ground-state rotational constants from infrared spectra and computed α, ref 12.

in another, closely related one, it makes sense to determine scale factors for the individual types of internal coordinate that are common to both molecules. This approach was recently applied by one of us to the trans and gauche forms of 1,3-butadiene, using an MP2/6-31G* force field and refining to the frequencies of the trans species only.[13] A typical assumption in such an approach is that the same scale factor applies to different symmetry coordinates associated with the same type of internal coordinate.

If, however, the objective in scaling is to make the description of the normal coordinates as precise as possible, a more extensive scaling procedure is desirable. The determination of additional scale factors must, of course, be based only on reliable experimental data, the more of these, the better.[28] The most elaborate treatment of butadiene of this kind to date was that employed by Wiberg and Rosenberg, who refined all 24 scale factors for the diagonal symmetry force constants and, in addition, 4 off-diagonal ones.[22] These authors used frequency data from four symmetrically substituted isotopomers, namely parent (d_0), 2,3-d_2, 1,1,4,4-d_4 and d_6. The treatment due to Choi et al. throws light on the assumption of identical factors for a given type of symmetry coordinate.[32] Such an assumption in the case of BDE would entail, for example, identical scale factors for the A_g and B_u symmetry force constants involving C=C stretching. Since the difference between these two constants depends solely on the valence interaction force constant f', the above assumption implies that the particular QC force field has determined f' perfectly. However, Choi et al. showed that this particular constant varies appreciably from one QC method to another, though not greatly with the basis set.[32] Not all of the resulting f' values can therefore be correct. The present investigation therefore identifies a general need for allowing the possibility of independent scale factors in the A_g and B_u versions of a particular type of symmetry coordinate, assuming, of course, that the values of interaction force constants concerned[33] are sensitive to the experimental data.

Our own objective was a procedure similar to that of Wiberg and Rosenberg.[22] However, we were limited by the ability of ASYM40 to refine independently only scale factors for the diagonal force constants, those for the off-diagonal ones being constrained to the geometric mean of the factors for the two corresponding diagonal constants, as in the procedure recommended by Pulay et al.[34] and given some theoretical justification by Pupyshev et al.[35] Alteration of individual off-diagonal constants is always possible, prior to refinement, and this proved necessary in one instance (see below). However, we were able to investigate the validity of the assumption of the constancy of scale factors for coordinates such as C=C stretching by refining independent scale factors for all but one of the 18 symmetry coordinates that do not involve CH stretching. (The scaling of the CH stretching constants is considered in detail below.) The set of symmetry coordinates employed, which mirror closely those in ref 13, is contained in Table 2.

A further concern in our approach to scaling was to use as far as possible only gas-phase data to reduce the uncertainty arising from frequency shifts upon change of phase. Doing so proved feasible in the in-plane vibrational problem, due to the existence of Raman gas-phase data for the A_g frequencies of the d_0, 2,3-d_2, 1,1,4,4-d_4, and d_6 isotopomers. The gas-phase data from the less symmetric isotopomers were not used in this refinement due to the risk of inverting the order of near-coincident frequencies such as ν_6 and ν_{22} in d_0 in a refinement that merges A_g and B_u motions into a single A′ symmetry class. However, this extended refinement was explored as described below.

By contrast, the absence of gas-phase data for the weak Raman-active B_g vibrations meant that both gas and liquid data had to be used in treating the out-of-plane modes. However, for the latter we were able to improve on previous treatments by including data from the parent and 10 deuterated isotopomers for which data are available, including those having only C_s symmetry. The latter offer the advantage of providing infrared gas-phase data for vibrational motions related to those in a symmetrical isotopomer, which are Raman active only. In the resulting A″ ($A_u + B_g$) refinement, the frequency order inversion problems among the C_s isotopomer data proved to be trivial.

Interpretation of the ν_{CH} and ν_{CD} Regions. Ideally a separate scale factor should be determined for the stretching of each type of CH bond present.[36] There is no reason or evidence available to suppose that any QC method will yield precisely the sequence of bond strengths involved or their anharmonicities, which are also involved in the scale factors. Such a scaling would be feasible were individual ν^{is}(CH) values to be available [36] which, hopefully, would be unaffected by the Fermi resonances which are so prevalent in the spectra of the normal species. However, such ν^{is}(CH) data are as yet lacking for BDE.

To determine a single scale factor for CH stretching, we need to choose frequencies which are least likely to be affected by Fermi resonances. Examination of the highest ν(CH) frequencies calculated from unscaled force fields for the d_0, 2,3-d_2, 2-d_1, *cis*- and *trans*-1-d_1, and 1,1,2-d_3 isotopomers showed that these coincided with each other within 1 cm^{-1}. Observation of gas phase infrared or Raman frequencies for these species consistently at 3099 ± 1 cm^{-1}, as listed in Table 3, then strongly

TABLE 2: Symmetry Coordinates for *trans*-1,3-Butadiene

motion type[a]	coordinate no. A_g	coordinate no. B_u	coordinate[b]
$\nu(CH_c)$	1	17	$r(C_1H_5) \pm r(C_4H_6)$
$\nu(CH_t)$	2	18	$r(C_1H_7) \pm r(C_4H_8)$
$\nu(CH_\alpha)$	3	19	$r(C_2H_9) \pm r(C_3H_{10})$
$\nu(C{=}C)$	4	20	$r(C_1C_2) \pm r(C_3C_4)$
$\nu(C{-}C)$	5		$r(C_2C_3)$
$\delta_s(CH_2)$	6	21	$\{2(\angle(H_7C_1H_5)) - \angle(H_5C_1C_2) - \angle(H_7C_1C_2)\} \pm \{2(\angle(H_6C_4H_8)) - \angle(H_6C_4C_3) - \angle(H_8C_4C_3)\}$
$\delta(CH_\alpha)$	7	22	$\{\angle(H_9C_2C_1) - \angle(H_9C_2C_3)\} \pm \{\angle(H_{10}C_3C_4) - \angle(H_{10}C_3C_2)\}$
$\rho(CH_2)$	8	23	$\{\angle(H_5C_1C_2) - \angle(H_7C_1C_2)\} \pm \{\angle(H_6C_4C_3) - \angle(H_8C_4C_3)\}$
δ_{skel}	9	24	$\angle(C_1C_2C_3) \pm \angle(C_2C_3C_4)$

motion type[a]	coordinate no. A_u	coordinate no. B_g	coordinate[b]
$w(CH_2)$	10	14	$op(C_1H_7H_5C_2) \pm op(C_4H_8H_6C_3)$
$w(CH_\alpha)$	11	15	$op(C_2C_1C_3H_9) \pm op(C_3C_4C_2H_{10})$
$\tau(CH_2)$	12	16	$\{\tau(H_5C_1C_2C_3) + \tau(H_5C_1C_2H_9) + \tau(H_7C_1C_2H_9) + \tau(H_7C_1C_2C_3)\} \pm \{\tau(H_6C_4C_3C_2) + \tau(H_6C_4C_3H_{10}) + \tau(H_8C_4C_3H_{10}) + \tau(H_8C_4C_3C_2)\}$
τ_{skel}	13		$\tau(H_9C_2C_3C_4) + \tau(C_1C_2C_3C_4) + \tau(H_{10}C_3C_2C_1) + \tau(H_{10}C_3C_2H_9)$

[a] The three types of CH bond are respectively cis (CH_c), trans (CH_t), and α (CH_α) with respect to the second $CH{=}CH_2$ group [b] The ± option involves using the plus sign for the A_g and A_u species, the minus sign for B_u and B_g. "*op*" and "*τ*" describe out-of-plane and dihedral angle bending coordinates, respectively.

suggests that the overall effects of Fermi resonance on these highest ν(CH) levels are small or negligible. This interpretation was reinforced by the quite good agreement found between observed and calculated ^{13}C shifts on these levels, as shown in Table 4. Our approach was therefore to scale the ν(CH) force constants to these observed frequencies near 3100 cm^{-1} using a single factor for all three types of CH bond. This treatment was carried out in conjunction with a 10-parameter scaling of the other types of A′ force constant as described below. Table 3 shows the resulting scaled frequencies from the dcct and mcct calculations, together with some predicted *unscaled* infrared intensities and Raman scattering activities.

Also shown in Table 3 are the potential energy distributions (PED) for the various CH(D) stretching modes. The latter are given in terms of the contributions from the three types of CH bond. The results of both B3LYP and MP2 calculations are quoted since these differ significantly in certain cases. These differences can be traced to a marked difference in the value of the ν(CH)/ν(CH) interaction force constant f'_{gem} which acts between the CH bonds sharing a common carbon atom. Unscaled values of these and other valence interaction force constants are shown in Table 5. Such differences in f'_{gem} are found quite generally and qualitative evidence has been advanced to support the B3LYP results.[37] The smaller MP2 value of f'_{gem} leads to a greater separation between higher frequency, antisymmetric stretching and lower frequency, symmetric stretching motion.

In the case of BDE, the PED's of Table 3 show that the MP2 and B3LYP results agree in showing that the modes near 3100 cm^{-1} (ν_1, ν_{17}) are composed of roughly $^2/_3\nu(CH_t)$ and $^1/_3\nu(CH_c)$ stretching motions. Though the contributions from these motions are out of phase, as seen from the normal coordinates (not shown), the modes hardly deserve their conventional description as "asymmetric CH_2 stretching" motions. The lower modes, ν_2, ν_3, ν_{18}, and ν_{19}, are then, roughly, mixtures of in-phase $\nu(CH_t)$/$\nu(CH_c)$ motion with stretching of the CH_α bonds. It is here that the MP2 and B3LYP descriptions tend to diverge markedly. The larger $\nu_{as}(CH_2)/\nu_s(CH_2)$ splitting from the MP2 calculation tends to bring about a closer coincidence with the intrinsically lower $\nu(CH_\alpha)$ frequency and therefore makes for greater coupling. However, in both treatments, the higher of these two frequencies, e.g., ν_2, is an in-phase motion of all three types of CH bond, which accounts for the high Raman scattering activity predicted for ν_2.

A further consequence of this difference in f'_{gem} between MP2 and B3LYP is its effect on the scaled value of f_{CH} for each bond and hence on their predicted ν^{is}(CH) values, which are listed at the bottom of Table 3. This is because scaling to the frequencies near 3100 cm^{-1} means that we are reproducing data which involve terms in f_{CH} *less* terms in f'_{gem}. The B3LYP values of f_{CH} then become larger than the MP2 ones, so that the B3LYP ν^{is}(CH) values tend to be slightly greater.

While as previously noted, no experimental data exist for the fundamental bands of the d_5 species, local mode frequencies $\nu_{lm} = \omega_{lm} - 2\omega x_{lm}$ for these species are available from the work of Kjaergaard et al.[20] The differing methodology used to determine these two types of quantity, ν_{lm} and ν^{is}(CH), means that absolute agreement between them is not to be expected. However, *differences* between the three types of CH bond might be expected to be the same. Table 3 shows that almost equal differences of 32−33 cm^{-1} appear for the $\Delta\nu_{lm}(CH_c{-}CH_\alpha)$ and $\Delta\nu_{lm}(CH_t{-}CH_c)$ pairs from the local mode data, whereas the corresponding $\Delta\nu^{is}$(CH) differences are 32−33 cm^{-1} for the $CH_c{-}CH_a$ pair but 22−25 cm^{-1} for the $\Delta\nu(CH_t{-}CH_c)$ pair. (These ν^{is}(CH) differences correlate with the bond length differences of Table 1). If the local mode data can be trusted, this result indicates a need for differing scale factors for CH_t and CH_c stretching. The quoted precisions of the local mode ω values are low,(CH_t, ± 4 cm^{-1}; CH_c ±10 cm^{-1}; CH_α ± 4 cm^{-1}),[20] a feature which may indicate considerable error in their differences. However, it may be questioned whether the above errors should be treated as independent of each other.

The only data in the fundamental region that might throw light on this question of scale factor variation are the ν^{is}(CD) values observed in the 2-d_1, *cis*-1-d_1, and *trans*-1-d_1 isotopomers. However, before any ν(CD) data can be utilized, our quadratic force field calculations have to be adapted to handle the differing effect of anharmonicity on CH and CD bond stretching. In Table 3, the expedient is employed of multiplying ν(CD) values calculated from force constants refined to ν(CH) values by the fudge factor 1.011 before comparing them with observed data.[14,38−41] The resulting calculated ν^{is}(CD) values agree within 3−6 cm^{-1} with those observed for the *cis* and *trans*-1-d_1 species, but they are about 9 cm^{-1} too high in the case of the 2-d_1

TABLE 3: Calculated Vibrational Data for Isotopomers of *trans*-1,3-Butadiene in the ν(CH) and ν(CD) Regions

							PED (dcct/mcct)[f]		
isotopomer	mode[a]	ν_{obsd}[b]	ν_{sc}(dcct)[c]	ν_{sc}(mcct)[c]	A_{un}[d]	R_{un}[e]	$\nu(CH_c)$	$\nu(CH_t)$	$\nu(CH_\alpha)$
parent	ν_1 A_g	*3100*[g] g	3099.9	3099.8		171	34/38	66/62	1/1
	ν_2 A_g	3012[g,h] g	3019.3	3012.3		307	60/32	25/11	15/56
	ν_3 A_g	?	3007.0	3001.5		57	6/31	9/26	85/43
	ν_{17} B_u	*3099.7*[h,i] g	3100.3	3100.1	25		34/37	65/62	2/1
	ν_{18} B_u	**3026**[g,h] g	3019.5	3016.8	8		24/13	4/2	72/85
	ν_{19} B_u	3011.4[g] g	3016.7	3004.0	24		42/50	31/36	26/14
1,4-$^{13}C_2$	ν_1 A_g		3087.5	3087.2		173	33/37	67/63	1/1
	ν_2 A_g		3014.1	3009.8		334	50/17	17/3	33/80
	ν_3 A_g		3005.9	2997.7		34	17/46	17/34	66/20
	ν_{17} B_u	3091[j] m	3088.0	3087.6	25		33/36	65/62	2/2
	ν_{18} B_u	3026[j] m	3018.6	3015.7	16		3/7	1/0	97/93
	ν_{19} B_u	2999[j] m	3011.2	2998.6	15		64/57	34/38	1/5
2,3-$^{13}C_2$	ν_1 A_g	**3090**[k] l	3099.7	3099.7		172	35/38	66/62	1/1
	ν_2 A_g	**2995**[k] l	3018.3	3008.5		270	64/54	31/27	4/19
	ν_3 A_g	?	2998.8	2995.7		95	1/9	4/11	96/81
	ν_{17} B_u	**3098.9**[k] g	3100.1	3100.0	24		35/37	65/62	1/1
	ν_{18} B_u	**3020**[h,k] g	3017.5	3009.5	10		66/37	32/14	1/49
	ν_{19} B_u	?	3009.4	3001.6	22		0/26	3/24	97/50
1-$^{13}C_1$	ν_1 A'	**3099**[l] g	3100.1	3100.0	13	83	34/37	65/62	1/1
	ν_2 A'	**3085**[l] g	3087.7	3087.4	12	90	33/36	66/63	2/2
	ν_3 A'	**3022**[h,l]g	3019.4	3016.3	6	87	33/11	10/1	57/87
	ν_4 A'	**3001**[l] l	3017.8	3011.1	15	130	30/25	18/8	51/69
	ν_5 A'	**3005**[l] g	3012.6	3002.7	11	111	56/41	27/31	17/28
	ν_6 A'	?	3006.4	2998.1	0	39	14/50	25/35	72/15
2,3-d_2	ν_1 A_g	*3098*[g] g	3099.0	3099.0		175	35/38	66/62	0/0
	ν_2 A_g	3005[g] g	3017.5	3006.2		211	62/62	34/38	0/0
	ν_3 A_g	2250[g] g	2251.6	2254.3		71	0/0	0/0	98/97
	ν_{17} B_u	*3098.6*[g] g	3098.9	3099.0	19		35/38	66/63	0/0
	ν_{18} B_u	**3016**[g,h] g	3017.5	3005.8	13		65/62	34/37	0/0
	ν_{19} B_u	2242.5[m] g	2253.4	2252.1	13		0/0	0/0	98/98
c,*c*-1,4-d_2	ν_1 A_g	3063[n] l	3074.6	3068.5		241	0/0	97/97	2/3
	ν_2 A_g	3017[n] l	3008.2	3006.7		132	0/0	3/3	98/98
	ν_3 A_g	2257[n] l	2269.0	2267.1		72	98/97	0/0	0/0
	ν_{17} B_u	3076[n] g	3074.7	3068.8	16		0/0	97/96	3/4
	ν_{18} B_u	3029[n] g	3018.5	3014.1	21		0/0	3/4	97/96
	ν_{19} B_u	2265[n] g	2269.0	2266.5	10		98/97	0/0	0/0
t,*t*-1,4-d_2	ν_1 A_g	**3039**[g] l	3048.5	3044.8		142	100/99	0/0	0/0
	ν_2 A_g	3006[n] l	3009.8	3008.6		171	0/0	0/0	100/0
	ν_3 A_g	2275[n] l	2287.5	2283.7		71	0/0	98/97	0/0
	ν_{17} B_u	3047.5[n] g	3049.5	3044.7	29		96/98	0/0	4/2
	ν_{18} B_u	3019[n] g	3019.2	3016.0	17		4/2	0/0	96/98
	ν_{19} B_u	2284.2[n] g	2290.3	2286.0	3		0/0	97/97	0/0
1,1,4,4-d_4	ν_1 A_g	3012[g] g	3010.0	3008.7		152	0/0	0/0	101/100
	ν_2 A_g	2318[g] g	2334.3	2335.9		79	42/43	59/58	0/0
	ν_3 A_g	2225[g] g	2228.4	2222.3		60	56/55	39/40	0/0
	ν_{17} B_u	3020.4[g] g	3020.4	3016.4	26		0/0	0/0	100/100
	ν_{18} B_u	2334.7[g] g	2333.5	2335.3	10		40/42	61/59	0/0
	ν_{19} B_u	2225.5[g] g	2231.8	2224.8	4		58/56	37/38	0/0
d_6	ν_1 A_g	**2336**[g,h] g	2334.7	2336.2		76	40/42	60/58	0/0
	ν_2 A_g	**2263**[g,h] g	2260.2	2263.0		128	16/13	5/5	74/78
	ν_3 A_g	**2224**[g,h] g	2218.5	2212.3		11	42/43	33/35	24/20
	ν_{17} B_u	**2342**[g,h] g	2334.6	2336.2	13		38/40	61/60	1/1
	ν_{18} B_u	2266.1[g] g	2261.7	2262.8	4		19/18	4/5	72/72
	ν_{19} B_u	2218.4[g] g	2221.6	2212.2	10		41/41	32/33	25/25
c,*t*-1,4-d_2	ν_1 A'	3067[o] g	3074.6	3068.7	8	120	0/0	97/96	3/3
	ν_2 A'	3036[n] l	3048.9	3044.7	15	69	98/99	0/0	2/1
	ν_3 A'	3020[o] g	3018.9	3015.2	19	7	2/1	2/2	96/98
	ν_4 A'	3006[o] l	3009.0	3007.5	0	146	0/0	2/2	99/99
	ν_5 A'	2284[n] g	2289.1	2284.9	1	35	1/1	97/97	0/0
	ν_6 A'	2265[n] g	2268.9	2266.7	5	36	98/97	1/1	0/0
2-d_1	ν_1 A'	*3100*[p] g	3100.1	3100.0	13	78	34/37	65/62	1/1
	ν_2 A'	3092[p] l	3098.9	3099.0	9	95	35/38	66/62	0/0
	ν_3 A'	3001[p] l	3019.3	3014.3	1	253	53/21	21/6	25/73
	ν_4 A'	3012[p] g	3017.5	3006.0	11	16	65/62	34/37	0/0
	ν_5 A'	?	3012.0	3003.1	10	19	13/42	14/33	74/26
	ν_6 A'	2244[p] g	2252.6	2253.3	6	36	0/0	0/0	98/98
t-1-d_1	ν_1 A'	*3100*[q] g	3100.1	3100.0	13	85	34/37	65/62	1/1
	ν_2 A'	3048[q] g	3048.9	3044.7	15	71	98/99	0/0	2/1
	ν_3 A'	3021[q] g	3019.5	3016.5	8	43	27/10	6/1	67/89
	ν_4 A'	?	3018.0	3010.6	16	139	37/19	22/8	40/74
	ν_5 A'	3003[q] s	3008.3	3002.5	1	87	5/36	6/29	90/36
	ν_6 A'	2286[q] g	2289.0	2284.9	1	35	0/0	98/99	0/0

TABLE 3: Continued

isotopomer	mode[a]	ν_{obsd}[b]	ν_{sc}(dcct)[c]	ν_{sc}(mcct)[c]	A_{un}[d]	R_{un}[e]	PED (dcct/mcct)[f] $\nu(CH_c)$	$\nu(CH_t)$	$\nu(CH_\alpha)$
c-1-d_1	ν_1 A′	*3099*[q] g	3100.1	3100.0	12	85	34/37	65/63	1/1
	ν_2 A′	3078[q] g	3074.6	3068.7	8	122	0/0	97/96	3/3
	ν_3 A′	3049[q] g	3019.5	3015.9	6	84	32/12	9/3	59/85
	ν_4 A′	?	3017.6	3009.4	20	79	30/17	22/11	48/72
	ν_5 A′	2995[q] g	3007.6	3002.3	0	84	4/33	7/28	90/39
	ν_6 A′	2263[q] g	2269.0	2266.8	5	36	98/98	0/0	0/0
1,1,2-d_3	ν_1 A′	*3098.1*[p] g	3100.1	3100.0	12	85	34/37	65/62	1/1
	ν_2 A′	3029.6[p] g	3019.0	3014.2	3	160	55/21	21/5	22/72
	ν_3 A′	2997[p] l	3012.3	3003.1	14	22	10/42	13/33	77/26
	ν_4 A′	2342.2[p] g	2334.6	2336.2	6	37	39/41	61/59	1/1
	ν_5 A′	2265.1[p] g	2261.1	2263.0	2	65	17/15	5/5	75/75
	ν_6 A′	2216.8[p] g	2220.1	2212.3	5	6	41/42	32/34	24/22
$(\nu^{is}(CH)_t)$[r]	ν_1 A′	(3061)[s]	3073.1	3066.8	6	111	0	100/100	0
$(\nu^{is}(CH_c))$[r]	ν_1 A′	(3028)[s]	3048.2	3044.4	10	80	100/100	0	0
$(\nu^{is}(CH)_\alpha)$[r]	ν_1 A′	(2996)[s]	3015.2	3012.6	13	75	0	0	100/100
	$\Delta\nu^{is}_{t-c}$	33	24.9	22.4					
	$\Delta\nu^{is}_{c-\alpha}$	32	33.0	31.8					

[a] For the asymmetric (C_s) isotopomers, modes are numbered in order of descending frequency. [b] Units in cm^{-1}: g = gas, l = liquid, m = argon matrix, and s = solid. In italics, frequencies selected for the single scale factor refinement; in boldface, new or significantly revised observations. [c] Units in cm^{-1}, from QC force constants scaled (one factor) on selected ν(CH) values. Calculated ν(CD) values are multiplied by 1.011. [d] Unscaled infrared intensity (km mol^{-1}) (dcct). [e] Unscaled Raman scattering activity (amu $Å^{-4}$) (dcct). [f] Potential energy distribution in terms of valence force constants for the stretching of CH bonds respectively cis (c), trans (t), or α to the vinyl group. For the C_s isotopomers, each term is the sum of contributions from both A_g and B_u symmetry coordinates. dcct and mcct values are separated by /. [g] This work. [h] Adjusted for Fermi resonance. [i] Reference 43. [j] Matrix frequencies from ref 44. Additional weak bands suggest Fermi resonances throughout. [k] Reference 6. [l] Data from ref 6. The modes ν_1 and ν_2 occur almost wholly in the $^{12}CH_2$═C and $^{13}CH_2$═C units respectively, the slight coupling between the two in the parent molecule having been completely removed by the ^{13}C substitution. Only ν_6 approximates to an A_g mode. [m] Reference 3. [n] Reference 5. [o] Reference 45. [p] Reference 13. [q] Reference 46. [r] Calculated for the appropriate d_5 species. [s] Local mode frequency ($\omega^{is}{}_{lm} - 2\omega x^{is}{}_{lm}$) from ref 20.

TABLE 4: Comparison of Observed and Calculated ^{13}C Isotope Frequency Shifts (cm^{-1}) for *trans*-1,3-Butadienes

			1,4-$^{13}C_2$			2,3-$^{13}C_2$			1-$^{13}C_1$		
		parent		$\Delta\nu_{sc}$[d]			$\Delta\nu_{sc}$[d]			$\Delta\nu_{sc}$[d]	
mode		ν_{obsd}[a]	$\Delta\nu_{obsd}$[b,c]	dcct*	mcct	$\Delta\nu_{obsd}$[b,e]	dcct*	mcct	$\Delta\nu_{obsd}$[b,f]	dcct*	mcct
A_g	ν_1	3091 l	?	12.4	12.6	1	0.1	0.1	11[g]	12.1	12.4
	ν_2	3002 l	?	5.1	2.5	7	1.0	3.8	1	1.4	1.2
	ν_3	?	?	1.1	3.8	?	8.1	5.8	?	0.6	3.4
	ν_4	1638 l	?	17.4	17.0	32	33.6	34.1	5	6.6	6.5
	ν_5	1438 l	?	3.2	3.3	10	8.8	8.7	1	1.7	1.7
	ν_6	1285* l	?	8.7	8.0	7*	7.4	7.7	5	7.5	7.4
	ν_7	1202 l	?	2.5	2.4	21	20.9	20.2	0	1.3	1.2
	ν_8	889 l	?	7.7	7.7	10	10.7	10.4	2	3.9	3.9
	ν_9	513 l	?	8.9	8.9	5	5.6	5.4	2	4.4	4.4
B_u	ν_{17}	3100.6 g	15	12.3	12.5	1.7	0.2	0.1	1.6	0.2	0.2
	ν_{18}	3026* g	?	1.0	1.1	7*	2.0	7.2	4	0.1	0.5
	ν_{19}	3011 g	?	5.5	5.3	?	7.3	2.3	?	4.2	1.3
	ν_{20}	1596.4 g	25	27.0	27.1	18.6	18.5	18.7	14.4	15.4	15.4
	ν_{21}	1380.6 g	0	1.0	1.0	13	13.1	12.9	0.6	0.5	0.5
	ν_{22}	1281* g	1*	6.7	7.5	6*	5.8	6.6	1	0.2	0.4
	ν_{23}	990 g	5	5.4	5.2	1	1.1	1.1	2	2.6	2.6
	ν_{24}	299 g	?	2.8	2.7	3	4.1	4.1	1	1.4	1.4
A_u	ν_{10}	1013.8 g	1	0.0	0.0	3.4	3.3	3.2	0	0.0	0.0
	ν_{11}	908.1 g	8	9.0	8.9	0.7	1.0	0.7	8	7.3	7.9
	ν_{12}	524.6 g	0	0.1	0.4	−0.3	1.4	1.3	0.1	0.1	0.1
	ν_{13}	162.4 g	?	1.9	1.9	1.4	2.4	2.4	0.4	0.9	1.0
B_g	ν_{14}	966 l	?	0.9	0.2	6	5.8	5.5	−2	0.4	0.1
	ν_{15}	908 l	?	8.2	8.7	0	0.5	1.0	2	1.4	0.9
	ν_{16}	749 l	?	0.0	0.1	9	13.0	12.9	−3	0.0	0.1

[a] ν(observed) $incm^{-1}$, this work; g = gas, l = liquid. Asterisks identify situations where a correction has been made for Fermi resonance.. [b] Observed fall in frequency due to ^{13}C substitution. [c] Argon matrix shift from ref 44. [d] Frequency shift from the scaled B3LYP/cc-pVTZ force field (dcct*) ($F_{11,12}$ preset to 0.0135 aJ rad^{-2}) or the MP2/cc-pVTZ force field (mcct). [e] Reference 6. [f] Reference 5. [g] The gas-phase shift is 15 cm^{-1}.

isotopomer. The observed ν^{is}(CD) bands may of course themselves be subject to unidentified Fermi resonances.

While no judgment on the question of variable ν_{CH} scale factors can therefore yet be passed, it is satisfactory to find broad agreement on the relative strengths of the three types of CH bond between unscaled QC calculations, observed ν^{is}(CD) values and local mode frequencies.

We now scrutinize individual spectra in order to reassess assignments and identify Fermi resonances.

d_0, 2,3-$^{13}C_2$, 1-$^{13}C_1$. In the infrared spectrum of d_0, a very small effect of resonance on the band at 3100.6 cm^{-1} has previously been diagnosed.[43] However, three bands at 3055, 3011, and 2984 cm^{-1}, when only two are expected, indicate the presence of a strongly interacting dyad or triad of levels. If

TABLE 5: Some Unscaled Valence Interaction Force Constants in *trans*-1,3-Butadiene[a]

		B3LYP			MP2	
type	bonds	dtz+	dcct	dcct+	mtz+	mcct
ν(CH)/ν(CH)	C_1H_c/C_1H_t[b]	0.0291	0.0334	0.0351	0.0086	0.0120
	C_1H_c/C_2H_α	−0.0045	−0.0041	−0.0038	−0.0040	−0.0031
	C_1H_t/C_2H_α	0.0124	0.0127	0.0124	0.0103	0.0115
	C_1H_c/C_4H_c	−0.0002	−0.0002	0.0001	0.0002	0.0002
	C_1H_t/C_4H_t	0.0019	0.0019	0.0021	0.0017	0.0016
	C_2H_α/C_3H_α	−0.0013	−0.0006	−0.0003	−0.0003	0.0002
	C_1H_c/C_3H_α	0.0092	0.0096	0.0092	0.0067	0.0060
	C_1H_t/C_3H_α	−0.0011	−0.0013	−0.0011	−0.0031	−0.0026
ν(C═C)/ν(C═C)		−0.1409	−0.1441	−0.1393	−0.1067	−0.1117
ν(C═C)/ν(C−C)		0.4861	0.5003	0.5029	0.4166	0.4335
$\delta(CH_2)/\delta(CH_2)$		0.0003	0.0004	0.0004	0.0003	0.0005
δ(CH)/δ(CH)		0.0402	0.0403	0.0401	0.0405	0.0408
$\rho(CH_2)/\rho(CH_2)$		0.0042	0.0043	0.0042	0.0051	0.0051
$\delta_{skel}/\delta_{skel}$		0.1478	0.1486	0.1490	0.1608	0.1651

[a] Units: ν / ν in aJ Å^{-2}: ∠/∠ in aJ rad^{-2} . [b] f'_{gem} as in text.

3055 and 2984 cm^{-1} represent a dyad, their intensity distribution, assuming no intrinsic intensity in the combination level, places ν_{18} at 3026 cm^{-1}. This value for ν_{18} lies within 7 cm^{-1} of the dcct prediction of 3019.5 cm^{-1}. The fundamental ν_{19}, left at 3011 cm^{-1}, is equally well fitted by both dcct and mcct predictions, which, however, are 12 cm^{-1} apart due to the difference in the above-mentioned f'_{gem} factor. Participation of ν_{19} in a triad could tip the balance either way.

In the 2,3-$^{13}C_2$ species, infrared bands at 3036 and 2988 cm^{-1} have been assigned as a dyad involving ν_{18}, with ν^0_{18} estimated at 3020 cm^{-1}, leaving ν_{19} unassigned.[6] The unperturbed ^{13}C shift on ν_{18} is then 6 cm^{-1}, in good agreement with the mcct prediction of 7.2 cm^{-1} (Table 4). Using 3020 cm^{-1} for ν_{19} would give a substantial ^{13}C shift in the wrong direction. However, both B3LYP and MP2 calculations give much more infrared intensity to ν_{19} than to ν_{18}, and so this analysis must be questioned.

In the 1-^{13}C isotopomer, the infrared band at 3005 cm^{-1} attributed to ν_{19} yields a ^{13}C shift of 6 cm^{-1}, which fits better with the B3LYP predicted value of 4.2 cm^{-1}. The Fermi resonance corrected value of 3022 cm^{-1} for ν_{18} yields a shift of 4 cm^{-1} where both methods predict ∼0.5 cm^{-1}. However, this difference lies within the likely errors in the resonance corrections.

In the d_0 A_g species, the problem is to assign ν_2 and ν_3. As mentioned above, in keeping with its in-phase composition, ν_2 should be far more intense in the Raman effect than ν_3. The strong Raman band at 3012 cm^{-1} (gas) or 3002 cm^{-1} (liquid) must then be assigned to ν_2, with ν_3 lying unobserved 12−16 cm^{-1} below. A possible very weak shoulder at 2987 cm^{-1} in the liquid may be due to ν_3. A ^{13}C shift of 7 cm^{-1} is then seen on passing to the liquid-phase Raman band observed at 2995 cm^{-1} in the 2,3-$^{13}C_2$ isotopomer. This would appear to be better fitted by the mcct shift of 3.8 cm^{-1} than the dcct one of 1.0 cm^{-1}. The mcct prediction for ν_2 of 3012 cm^{-1} is also better than the dcct one of 3019 cm^{-1}.

Both methods predict a larger ^{13}C shift on ν_3 (dcct, 8.1 cm^{-1}, mcct 5.8 cm^{-1}), but this finding need not constitute an argument for reassigning the Raman band in each isotopomer to ν_3. Instead, we draw attention to a possible source of additional ^{13}C shift in ν_2 from the presence of small Fermi resonances. Weak resonances involving ν_2 are possible with $2\nu_{20}$, seen above as a weak band at 3180 cm^{-1} and two similar bands below, 2953 cm^{-1} due to $\nu_{20} + \nu_{21}$ and 2870 cm^{-1} due to $2\nu_5$, all of these in the liquid phase. The combined effects of resonance with the levels above and below may well be to leave the value of ν_2 unchanged for the d_0 species. However, the ^{13}C shifts on these combination levels above and below are much larger than that on ν_2 in the d_0 species. In consequence a resonance with a level above will *increase* on ^{13}C substitution whereas the same effect from levels below *decreases*. The net effect will then be a transfer of additional ^{13}C shift to the perturbed value of ν_2 . While there currently appears to be no evidence for loss of ^{13}C shift in the 3180, 2953, and 2870 cm^{-1} bands, the possibility of such a transfer both here and in the infrared B_u bands suggests that evidence from ^{13}C shifts generally in this region should be viewed with great caution.

2,3-d_2. In the infrared, an obvious dyad, 3031.4 and 2972.4 cm^{-1}, yields an unperturbed value of ν_{18} of 3016 cm^{-1}, well reproduced by the dcct predictions, poorly by the mcct ones. However, ν_2 at 3005 cm^{-1} in the gas phase Raman spectrum is exactly reproduced by the mcct calculation, poorly so by the dcct one. Both methods indicate that ν_2 and ν_{18} should be nearly degenerate. It seems likely, therefore, that resonances here are either imperfectly analyzed or as yet unidentified. In the liquid Raman spectrum, the strong band due to ν_2 at 2995 cm^{-1} is accompanied by weak satellite bands at 2942 and 3041 cm^{-1} which might be expected to exert equal and opposite effects on ν_2, as is possible in d_0.

In the ν(CD) region, the dcct and mcct calculations agree on both the degeneracy and absolute positions of ν_3 and ν_{19}. The difference of 7.5 cm^{-1} between the observed values of ν_3 and ν_{19} therefore points to an unidentified resonance on one of these levels at least. That the observed value of 2250 cm^{-1} for ν_3 agrees with both dcct and mcct predictions may be an accidental consequence of an inadequate scale factor, as suggested by the too high a value both methods yield for ν_{19} (ν^{is}(CD)) in 2-d_1. Both ν_3 and ν_{19} should therefore be examined again for signs of resonance.

1,4-d_2 Species. The interpretation of the Raman spectra of the three 1,4-d_2 species, especially in the CH stretching region, is complicated by the mixing of these isotopomers in the sample preparations. Benedetti et al. did not consider this problem in the interpretation of their spectra.[45] In our spectra, the mixing of the 1,4-d_2 isotopomers was comparable. Using normal coordinate calculations to provide additional guidance for untangling this region, we have revised some of our previously reported assignments.[4]

cis,cis-1,4-d_2. In the infrared spectrum the bands at 3076 and 2265 cm^{-1} are well fitted by the predictions for ν_{17} and ν_{19}. However, ν_{18}, assigned to 3029 cm^{-1}, is at least 10 cm^{-1} higher than expected. The explanation may be a resonance with a weak additional band seen near 2900 cm^{-1}. The Raman modes ν_1 and ν_3 are well fitted by the liquid frequencies of 3063 and

2257 cm^{-1}, once reasonable gas/liquid shifts have been applied. The *cis,trans*- impurity will contribute to the former band. However, ν_2 presents a problem. Our *cis,cis*-1,4-d_2 sample contained also Raman bands at 3106, 3040, 3017, 3009, and 2975 cm^{-1}. Where previously we had assigned 3017 and 3009 cm^{-1} to a dyad involving ν_2, we now associate ν_2 only with 3017 cm^{-1} and consider the 3040 and 3009 cm^{-1} bands to arise from both *trans,trans*- and *cis,trans*- impurities. This view is supported by the apparent absence of 3009 cm^{-1} in the earlier Raman spectrum.[45] The band at 3106 cm^{-1} must be due to 1-d_1 impurity, as suggested previously by Benedetti et al.[45] These authors also attributed the 2975 cm^{-1} band to 1-d_1 impurity, but assignment instead to a dyad in the *cis,cis*- species involving ν_2 at 3017 cm^{-1} would help to explain why ν_2 then appears some 10 cm^{-1} higher than expected.

trans,trans-1,4-d_2. The small ν_3/ν_{19} splitting expected in the ν(CD) modes is rather well reproduced by observation once an appropriate gas/liquid shift of about 6−7 cm^{-1} has been applied to the liquid data. Infrared bands at 3047.5 and 3019 cm^{-1} agree excellently with the dcct predictions for ν_{17} and ν_{18}. The strongest Raman line at 3006 cm^{-1} (liquid) is in fair agreement with the dcct prediction of 3010 cm^{-1} for ν_2. For ν_1 we conclude that 3039 cm^{-1} is the correct assignment. However, both of the 3039 and 3006 cm^{-1} bands will have a *cis,trans*- component, while weaker bands at 3064 and 3020 cm^{-1} will derive entirely from a *cis,cis*-/*cis,trans*- mixture and *cis,cis*- impurities, respectively.

cis,trans-1,4-d_2. Since this isotopomer was present only as an impurity in our spectra, we will rely mainly on the earlier spectra.[45] Of the modes ν_1, ν_2, ν_3, and ν_4, we believe ν_1 to be represented by 3067 (IR, gas) and 3060 (Raman, liquid), ν_2 by 3036 cm^{-1} (Raman, liquid), ν_3 by 3020 cm^{-1}(IR, gas) and ν_4 by 3006 cm^{-1} (Raman, liquid). Of these four assignments, the last is somewhat higher than predicted, once a gas/liquid shift has been applied. The ν(CD) frequency ν_5 is clearly 2280 (IR, gas), 2274 cm^{-1} (Raman, liquid), while ν_6 is 2260 cm^{-1} (IR, gas), 2255 cm^{-1} (Raman, liquid). For ν_5 and ν_6 the more recent[4] values of 2284 and 2265 cm^{-1} are preferred (Table 3). The gas/liquid shifts implied here suggest some experimental error.

1,1,4,4-d_4. Fit to all predictions is generally good, except for ν_2. In the case of ν_{17} the agreement is likely to be due to cancellation between equal and opposite perturbations involving weak bands above and below the main infrared band at 3020.4 cm^{-1}. There are signs of similar perturbations affecting ν_1 in the Raman spectrum. ν_2 must contribute to a complex of weak Raman bands at 2353, 2328, and 2311 cm^{-1}(liquid), of which $2 \times \nu_6 = 2334$ and $\nu_4 + \nu_8 = 2349$ cm^{-1} are likely participants. Sensible estimates of perturbations associated with the latter bands lead to an unperturbed value for ν_2 of 2318 cm^{-1}in the gas, which is well below its expected value.

d_6. Four resonances are likely here. In the infrared, bands at 2349 and 2320 cm^{-1} suggest an unperturbed value for ν_{17} of 2342 cm^{-1}. Predicted values, however, suggest a somewhat lower value. All three Raman modes appear to be involved in resonance dyads. Thus, 2343 and 2330 cm^{-1} combine to give an unperturbed value of ν_1 of 2336 cm^{-1}, in excellent agreement with prediction. Similar pairs, 2265 with 2256 cm^{-1} and 2237 with 2212 cm^{-1}, give unperturbed values of ν_2 and ν_3 of 2263 and 2224 cm^{-1}. The latter may be too high, certainly if the mcct prediction is valid.

2-d_1. Once gas/liquid shifts have been taken into account, agreement with predictions is fair. It seems likely that ν_5 has not been observed, probably due to its proximity to the much stronger Raman band at 3001 cm^{-1} assigned to ν_3 (liquid). As mentioned previously, the ν^{is}(CD) mode ν_6 is predicted to be too high by 9 cm^{-1}.

trans-1-d_1. The four gas-phase frequencies available[46] appear to be well reproduced by the predictions. However, the additional band reported at 3072 cm^{-1} suggests a more complex situation.[46] A Raman spectrum will probably be needed to locate ν_4.

cis-1-d_1. The earlier assignments[46] of ν_3 and ν_5 to the infrared bands at 3049 and 2995 cm^{-1} look implausible. ν_3 should lie near 3020 cm^{-1}, and the infrared intensity of ν_5 should be very low. A Fermi resonance dyad involving ν_3 seems a better explanation for these two bands. Considerations of intensity also suggest that ν_4 should be obvious in the Raman spectrum, not as yet available.

1,1,2-d_3. Here also there are possible signs of resonance since Abe reports an infrared band in the gas phase at 3060 cm^{-1}, in addition to those at 3099, 3016, and 2995 cm^{-1}, assigned to ν_1, ν_2, and ν_3.[46] However, later estimates[13] of the frequencies of the last two of these bands − 3029.6 cm^{-1} (gas) and 2997 cm^{-1} (liquid) are different, suggesting an impurity problem in ref 46. In contrast, the two studies agree excellently on the three ν(CD) frequencies for ν_4, ν_5, and ν_6. Both the latter and the newer values of ν_2 and ν_3 (with a gas/liquid shift applied) are well reproduced by our scaled force fields.

In concluding this section, we believe that the present scaled force fields have achieved a relatively satisfactory description of the fundamental CH and CD stretching bands in the whole range of isotopomers. Further refinement must await experimental values of ν^{is}(CH), an exploration of the effects of anharmonicity and better harmonic force fields.

Overall Scaling of the A′ Force Field. Scale factor refinements were carried out for five force fields, B3LYP/6-311++G** ("dtz+"), B3LYP/cc-pVTZ ("dcct"), B3LYP/aug-cc-pVTZ)("dcct+"), MP2/6-311++G** ("mtz+"), and MP2/cc-pVTZ ("mcct"). The resulting factors are listed in Table 6. Apart from the single scale factor used for the six CH bond stretches, the joint A_g and B_u species contain another possible 11 factors. Of the latter, independent factors were refined in the two symmetry species except in the case of the CH_2 symmetric deformation motions ($\delta(CH_2)$), where interaction between motions located in the two ends of the molecule seemed rather unlikely. This idea was supported by the very small valence interaction constant f' values determined in the unscaled QC calculations, as seen in Table 5. Where significant interactions of this kind were found, as in the ν(C═C)/ν(C═C), δ(CH)/δ(CH) and $\delta_{skel}/\delta_{skel}$ motions, it seemed important to assign independent scale factors in the A_g and B_u species, as discussed above. Although the valence interaction between $\rho(CH_2)$ motions proved to be very small, it was thought advisable for independent scale factors to be retained here also.

The dispersions quoted are probably overestimated insofar as they are associated with uncertainties of 1% in all frequencies utilized in the refinements, which may be over generous. As the data stand, while the evidence for differing A_g and B_u scale factors for ν(C═C) stretching in the two MP2 force fields is fairly strong, in the case of the three B3LYP force fields, it is weak (Table 6). The largest A_g/B_u difference of nearly 5% is found with the mcct δ_{skel} scale factors. In all the doubtful situations, it seemed safer to opt for more rather than fewer independent factors.

Two scale factors are more poorly determined than the rest, those for ν(C−C) and $\rho(CH_2)$ in the A_g species. This deficiency is related to a high correlation between these two parameters.

TABLE 6: Scale Factors of the in Plane Vibrational Force Field for *trans*-1,3-Butadiene ($A' = A_g + B_u$)[a]

		MP2		B3LYP		
motion type	sym. coord. no.(s)	mtz+	mcct	dtz+	dcct	dcct+
ν(CH)	1, 2, 3, 17, 18, 19	0.8944(35)	0.8918(36)	0.9273(30)	0.9264(30)	0.9267(30)
ν(C═C) A_g	4	0.9336(68)	0.9214(70)	0.9252(56)	0.9176(54)	0.9229(54)
ν(C═C) B_u	20	0.9611(41)	0.9466(42)	0.9363(34)	0.9254(33)	0.9317(33)
$\Delta\nu$(C═C)[b]	4, 20	−0.0275(109)	−0.0252(112)	−0.0111(90)	−0.0078(87)	−0.0088(87)
ν(C−C) A_g	5	0.9211(120)	0.9168(124)	0.9615(105)	0.9592(103)	0.9609(103)
$\delta_s(CH_2)$	6, 21	0.9532(34)	0.9512(36)	0.9686(30)	0.9595(29)	0.9594(29)
$\delta(CH_\alpha)$ A_g	7	0.9637(57)	0.9719(61)	0.9608(48)	0.9543(48)	0.9572(48)
$\delta(CH_\alpha)$ B_u	22	0.9521(56)	0.9618(60)	0.9465(47)	0.9399(46)	0.9414(46)
$\Delta\delta(CH_\alpha)$[b]	7, 22	0.0116(113)	0.0101(121)	0.0143(95)	0.0144(94)	0.0158(94)
$\rho(CH_2)$ A_g	8	1.0029(129)	0.9956(132)	1.0017(110)	0.9877(107)	0.9872(106)
$\rho(CH_2)$ B_u	23	0.9827(52)	0.9804(55)	0.9795(44)	0.9683(43)	0.9699(43)
$\Delta\rho(CH_2)$[b]	8, 23	0.0202(181)	0.0152(187)	0.0222(154)	0.0194(150)	0.0173(149)
δ_{skel} A_g	9	1.0006(61)	1.0183(66)	0.9766(50)	0.9715(49)	0.9732(49)
δ_{skel} B_u	24	1.0346(37)	1.0657(40)	0.9991(30)	0.9924(30)	0.9945(29)
$\Delta\delta_{skel}$[b]	9, 24	−0.0340(98)	−0.0474(106)	−0.0225(80)	−0.0209(79)	−0.0213(78)
ΣWSE[c]		6.60	7.13	4.73	4.60	4.54

[a] Refined to the gas-phase frequencies of six symmetrical isotopomers. Symmetry coordinates 1−9, A_g; 17−24, B_u. Basis sets: tz+ = 6-311++G**, cct = cc-pVTZ, cct+ = aug-cc-pVTZ. In parentheses is given the dispersion. [b] Scale factor difference, $A_g - B_u$. [c] Sum of least squares of errors in frequencies. Uncertainties associated with frequencies utilized are, somewhat arbitrarily, ± 1%. Since all ν(CH) and ν(CD) predictions are made with the same single scale factor, the *spread* of such frequencies is virtually independent of the quoted scale factor error.

We then explored the possibility that greater precision here might result by including the gas-phase frequencies of the less symmetrical isotopomers in the scale factor refinement. This entailed the omission of the d_0 ν_6 and ν_{22} data. The new set of scale factors is reported in the Supporting Information, Table S1. The modest improvement found in the precision of the ν(C−C) and $\rho(CH_2)$ scale factors was not enough to justify adoption or further reporting of this wider procedure.

The relative merits of the different force fields can be assessed by comparing the weighted sums of squares of errors, ΣWSE, as listed at the bottom of Table 6. The B3LYP force fields provide better fits than the MP2 ones, and there is virtually no advantage in extending the basis set from cc-pVTZ (dcct) to aug-cc-pVTZ (dcct+).

Reproduction of A′ Frequencies below 2000 cm^{-1} and Fermi Resonances. . The dcct and mcct results were selected for comparison of observed and calculated scaled frequencies. Data for the fully symmetrical isotopomers are given in Table 7, along with PED's from the dcct calculation. Table 8 contains, for the asymmetric isotopomers, only the frequency comparison. Calculated ^{13}C isotope shifts are compared with those observed in a particular phase in Table 4. Unscaled QC infrared intensities and Raman activities are given in the Supporting Information, Tables S2 and S3. In all cases we number the modes in order of descending frequency in the appropriate symmetry species. In the case of the less symmetric isotopomers, we follow Abe[46] and differ from most past practice in assigning numbers in the above way to the A′ and A″ symmetry species of the C_s point group. As an aid to comparison with earlier numbering systems, letters *g* or *u* designate modes which from the PED are predominantly A_g or B_u in character.

Italics identify those observed frequencies selected for use in the refinements, and boldface type designates frequencies newly observed or significantly revised. Frequencies in parentheses are the dcct predicted values for fundamentals so far unobserved. We examine first the symmetric species in Table 7.

d_0. In the A_g species, the very mixed mode ν_6 at 1278 cm^{-1} in the gas-phase Raman spectrum has long been assumed to be in resonance with 1300 cm^{-1} above[13,49] and an unperturbed value of 1285 cm^{-1}, slightly lower than a previous estimate of 1291 cm^{-1},[13] was chosen. The dcct calculation favors 1285 cm^{-1}; the mcct one, 1291 cm^{-1}. The position of the analogous band, 1292 cm^{-1}, of the 2-d_1 molecule in the Raman spectrum[48] evidently supports the explanation of the high intensity of the 1300 and 1278 cm^{-1} bands in d_0 by Fermi resonance.

The fundamental ν_{22} is associated with the pair of infrared bands of the same shape and equal intensity at 1294 and 1268 cm^{-1}. The chosen unperturbed value of 1281 cm^{-1} is about 8 cm^{-1} lower than the dcct prediction, which is a little worrying.

However, a similar pair of bands is observed in the Raman spectrum of the 2-d_1 isotopomer,[43] and the presence of a resonance on ν_{22} seems unavoidable.

2,3-d_2. Resonances were identified in the case of ν_4 and ν_5. The unperturbed value of ν_4, 1620 cm^{-1}, was taken from the doublet 1624, 1614 cm^{-1} involving $2\nu_{15}$. A resonance between ν_5 and $\nu_7 + \nu_9$ is likely to be small and a correction of 2 cm^{-1} has been applied. The fit is barely affected by these corrections. In the B_u species, the observed datum 840 cm^{-1} quoted for ν_{23} was from a very uncertain feature and as such was withheld from the refinement. However, it was well reproduced by the dcct calculation.

cis,cis- and trans,trans-1,4-d_2. No resonances were identified in these two isotopomers. The liquid-state A_g data, not used in the refinement, were well fitted. The fundamental ν_{23} in the *trans,trans-* compound could not be detected in our study, due to the presence of the *cis,trans-* impurity band at 850 cm^{-1}. The previous value of 846 cm^{-1},[13] not used, is well fitted by our predictions.

1,1,4,4-d_4. Evidence for ν_8 was seen in our spectra only in the liquid (740 cm^{-1}). This value is well fitted. No resonances were seen.

d_6. The mixed mode ν_5 (ν_7 in ref 13) is associated with the pair of bands 1198 and 1178 cm^{-1}, from which an unperturbed value of 1191 cm^{-1} was obtained. This value was well fitted. A likely Q branch at 742 cm^{-1} under the R branch of ν_{11} was assigned to ν_{23}. This datum was used and well fitted.

We consider now the less symmetric isotopomers in Table 8.

cis,trans-1,4-d_2. The fundamental ν_{14}, previously placed at 850 cm^{-1} as mode number ν_{23} in different numbering,[13] is predicted to lie at 870 cm^{-1}. The C type band in this region

TABLE 7: Observed Frequencies and Frequency Fit for Six Fully Symmetrical Isotopomers of *trans*-1,3-Butadiene in the Region below 2000 cm^{-1}

		parent				2,3-d_2			
mode		ν_{obsd}[a,b]	ϵ_{dcct}[c]	ϵ_{mcct}[c]	PED[d] (dcct)	ν_{obsd}[a,b]	ϵ_{dcct}[c]	ϵ_{mcct}[c]	PED[d] (dcct)
A_g	ν_4	*1644*	−4.2	−5.5	$69S_4$, $16S_5$, $15S_6$, $22S_7$	**1620***	−4.1	−4.5	$72S_4$, $17S_5$, $20S_6$, $10S_7$
	ν_5	*1442*	−7.3	−5.3	$8S_5$, $76S_6$, $18S_7$	*1429**	−2.5	−1.2	$5S_4$, $12S_5$,$78S_6$, $6S_7$
	ν_6	***1285****	−2.3	−6.6	$20S_4$, $10S_6$, $33S_7$, $17S_8$, $10S_9$	*1220*	−4.3	−9.5	$7S_4$, $19S_5$, $44S_8$, $21S_9$
	ν_7	*1204*	−5.8	−6.7	$29S_5$, $26S_7$, $25S_8$, $15S_9$	*935*	0.4	0.9	$5S_4$, $78S_7$
	ν_8	*889*	1.3	2.8	$6S_4$, $45S_5$, $45S_8$	*882*	0.9	2.8	$7S_4$, $48S_5$, $41S_8$
	ν_9	*513*	1.7	1.6	$6S_4$, $6S_5$, $14S_8$, $73S_9$	*497*	0.3	0.8	$5S_4$, $6S_5$, $6S_7$, $14S_8$, $72S_9$
B_u	ν_{20}	*1596.45*[e]	−4.0	−4.1	$72S_{20}$, $35S_{21}$	*1586.0*	−3.9	−3.0	$68S_{20}$, $38S_{21}$
	ν_{21}	*1380.6*	−4.5	−4.2	$21S_{20}$, $65S_{21}$, $8S_{22}$	*1374.1*	−3.1	−3.4	$27S_{20}$, $63S_{21}$
	ν_{22}	***1281****	−7.5	−9.9	$8S_{20}$, $62S_{22}$, $15S_{23}$	*1127.3*	1.1	−3.8	$20S_{22}$, $62S_{23}$
	ν_{23}	*990*	0.5	2.7	$26S_{22}$, $78S_{23}$	**840**	3.0	7.3	$75S_{22}$, $32S_{23}$
	ν_{24}	*299*	0.5	0.3	$8S_{23}$, $98S_{24}$	*286.9*	−0.6	−0.7	$7S_{23}$, $98S_{24}$
A_u	ν_{10}	*1013.8*	−2.9	−6.2	$32S_{11}$, $60S_{12}$, $6S_{13}$	*908.04*[e]	−0.4	−1.0	$100S_{10}$
	ν_{11}	*908.07*[e]	−0.3	−0.1	$101S_{10}$	*852.0*	−1.7	0.7	$19S_{11}$, $77S_{12}$
	ν_{12}	*524.57*	0.1	0.5	$50S_{11}$, $41S_{12}$	*480.3*	2.1	1.0	$68S_{11}$, $24S_{12}$, $7S_{13}$
	ν_{20}	*162.42*[f]	−0.5	−0.2	$17S_{11}$, $89S_{13}$	*152.6*	−0.7	−0.7	$13S_{11}$, $93S_{13}$
B_g	ν_{14}	*966* l	1.6	0.0	$5S_{14}$, $63S_{15}$, $46S_{16}$	*913* l	−2.5	2.7	$101S_{14}$, $8S_{15}$
	ν_{15}	*908* l	−3.9	−2.1	$97S_{14}$, $6S_{16}$	**802** l	−2.5	−4.3	$23S_{15}$, $84S_{16}$
	ν_{16}	*749* l	−4.2	−5.3	$40S_{15}$, $49S_{16}$	*742* l	−3.5	−6.3	$69S_{15}$, $19S_{16}$

		c,c-1,4-d_2				*t,t*-1,4-d_2			
mode		ν_{obsd}[a,g]	ϵ_{dcct}[c]	ϵ_{mcct}[c]	PED[d] (dcct)	ν_{obsd}[a,g]	ϵ_{dcct}[c]	ϵ_{mcct}[c]	PED[d] (dcct)
A_g	ν_4	1620 l	−8.0	−8.8	$69S_4$, $18S_5$, $5S_6$, $27S_7$	1626 l	−4.2	−4.7	$67S_4$, $18S_5$, $7S_6$, $26S_7$
	ν_5	1378 l	−7.5	−7.1	$9S_5$, $50S_6$, $24S_7$, $14S_8$	1316 l	−5.6	−1.2	$55S_6$, $44S_7$
	ν_6	1225 l	−2.4	0.3	$11S_4$, $13S_5$, $9S_6$, $50S_7$, $6S_8$	1286 l	0.1	−4.4	$17S_4$, $22S_6$, $19S_7$, $22S_8$, $12S_9$
	ν_7	1122 l	−0.9	−6.3	$6S_4$, $23S_5$, $33S_6$, $9S_8$, $30S_9$	1170 l	−2.5	−5.2	$50S_5$, $8S_6$, $12S_7$, $10S_8$, $17S_9$
	ν_8	835 l	−0.3	1.3	$5S_4$, $38S_5$, $48S_8$	752 l	3.4	4.8	$7S_4$, $28S_5$, $9S_6$, $50S_8$
	ν_9	462 l	1.7	2.1	$5S_4$, $25S_8$, $67S_9$	501 l	1.6	1.8	$6S_4$, $18S_8$, $73S_9$
B_u	ν_{20}	*1559.3*	0.9	0.3	$86S_{20}$, $15S_{21}$, $6S_{22}$	1562	0.5	0.7	$81S_{20}$, $18S_{21}$, $6S_{22}$
	ν_{21}	*1328*	1.6	2.1	$41S_{21}$, $40S_{22}$, $15S_{23}$	1285	−8.3	−12.1	$14S_{20}$, $19S_{21}$, $36S_{22}$, $16S_{23}$
	ν_{22}	*1212.2*	3.6	4.3	$11S_{20}$, $36S_{21}$, $42S_{22}$	1243	−1.7	1.4	$55S_{21}$, $46S_{22}$
	ν_{23}	*862*	−0.2	0.1	$10S_{21}$, $13S_{22}$, $74S_{23}$, $5S_{24}$	[854.4]	0.0	0.7	$10S_{21}$, $13S_{22}$, $73S_{23}$, $5S_{24}$
	ν_{24}	**276**	0.3	0.3	$12S_{23}$, $95S_{24}$	277	0.9	1.0	$12S_{23}$, $95S_{24}$
A_u	ν_{10}	*995*	1.9	2.1	$12S_{10}$, $37S_{11}$, $50S_{12}$, $6S_{13}$	1002.55	0.0	−6.9	$7S_{10}$, $29S_{11}$, $52S_{12}$, $7S_{13}$
	ν_{11}	*808.37*	4.3	−2.8	$86S_{10}$	825.5	−1.0	3.8	$88S_{10}$, $19S_{11}$
	ν_{12}	*467*	−1.6	3.2	$47S_{11}$, $51S_{12}$	435	2.8	1.7	$6S_{10}$, $34S_{11}$, $48S_{12}$, $9S_{13}$
	ν_{13}	**153**	0.9	0.8	$14S_{11}$, $90S_{13}$	158	−0.8	−0.3	$19S_{11}$, $86S_{13}$
B_g	ν_{14}	*960* l	0.0	5.1	$20S_{14}$, $64S_{15}$, $34S_{16}$	*961* l	10.5	1.5	$60S_{15}$, $42S_{16}$
	ν_{15}	*818* l	3.2	−10.6	$64S_{14}$, $23S_{15}$	*862* l	−8.1	5.5	$77S_{14}$, $29S_{15}$, $7S_{16}$
	ν_{16}	*683* l	−2.9	4.9	$17S_{14}$, $17S_{15}$, $66S_{16}$	**602** l	−12.2	−16.7	$22S_{14}$, $14S_{15}$, $52S_{16}$

		1,1,4,4-d_4				d_6			
mode		ν_{obsd}[a,b]	ϵ_{dcct}[c]	ϵ_{mcct}[c]	PED[d] (dcct)	ν_{obsd}[a,b]	ϵ_{dcct}[c]	ϵ_{mcct}[c]	PED[d] (dcct)
A_g	ν_4	*1614*	−0.1	0.2	$65S_4$, $19S_5$, $29S_7$	1589	5.7	6.6	$73S_4$, $23S_5$, $14S_7$
	ν_5	*1299*	3.3	5.4	$19S_4$, $10S_6$, $61S_7$	1191*	4.3	2.5	$6S_4$, $40S_5$, $19S_6$, $10S_7$, $15S_8$, $15S_9$
	ν_6	*1169*	−4.4	−8.4	$50S_5$, $10S_7$, $15S_8$, $22S_9$	1048	0.2	−1.4	$65S_6$, $5S_7$, $10S_8$, $17S_9$
	ν_7	*1042*	0.9	0.2	$81S_6$, $8S_9$	920	2.3	2.9	$5S_4$, $6S_5$, $8S_6$, $69S_7$
	ν_8	740 l	1.8	3.2	$7S_4$, $29S_5$, $51S_8$	740	3.0	4.6	$7S_4$, $30S_5$, $49S_8$
	ν_9	*454*	0.7	1.2	$5S_4$, $28S_8$, $67S_9$	440	−1.3	−0.4	$5S_7$, $28S_8$, $67S_9$
B_u	ν_{20}	*1532.7*	3.0	3.3	$86S_{20}$, $8S_{21}$, $7S_{22}$	1519.7	4.7	5.7	$87S_{20}$, $9S_{21}$
	ν_{21}	*1267.3*	2.1	2.8	$81S_{22}$, $5S_{23}$	1048.2	3.9	4.1	$57S_{21}$, $28S_{22}$, $10S_{23}$
	ν_{22}	*1030.0*	5.6	5.7	$5S_{20}$, $91S_{21}$	1005.4	7.1	4.2	$5S_{20}$, $35S_{21}$, $25S_{22}$, $18S_{23}$
	ν_{23}	*812.7*	−2.3	−2.1	$13S_{22}$, $81S_{23}$, $7S_{24}$	742	2.0	4.9	$44S_{22}$, $59S_{23}$
	ν_{24}	*257.9*	0.1	0.2	$15S_{23}$, $93S_{24}$	249	−1.2	−1.0	$14S_{23}$, $94S_{24}$
A_u	ν_{10}	*955.4*	2.9	−2.9	$47S_{11}$, $44S_{12}$, $8S_{13}$	764.7	2.1	3.9	$27S_{10}$, $40S_{11}$, $38S_{12}$
	ν_{11}	*728.2*	1.0	2.1	$98S_{10}$	718.3	1.8	−1.0	$72S_{10}$, $17S_{12}$
	ν_{12}	*396.8*	0.8	2.6	$37S_{11}$, $57S_{12}$	384	1.4	2.6	$48S_{11}$, $47S_{12}$
	ν_{13}	*149.2*[h]	−0.1	−0.1	$16S_{11}$, $88S_{13}$	141.7[h]	0.8	0.5	$12S_{11}$, $92S_{13}$
B_g	ν_{14}	*930* l	−0.1	−1.5	$87S_{15}$, $22S_{16}$	798	−1.0	9.0	$34S_{14}$, $81S_{15}$
	ν_{15}	*727* l	−0.1	1.1	$90S_{14}$, $13S_{16}$	*702* l	6.4	−1.8	$64S_{14}$, $17S_{15}$, $13S_{16}$
	ν_{16}	*608*[i]	0.1	−0.3	$9S_{14}$, $15S_{15}$, $65S_{16}$	605?[j]	9.3	9.3	$5S_{15}$, $85S_{16}$

[a] Wavenumber units (cm^{-1}) observed in gas, except where otherwise indicated. l = liquid. Asterisks indicate frequencies corrected for Fermi resonances. In italics, data employed in the scale factor refinements. Liquid values were so employed only in the A″ species. Values given with two-decimal-place significance are from analysis of rotational structure. Significantly revised values are in boldface. Calculated (dcct) values in square brackets. [b] This work, except where otherwise indicated. [c] Frequency fit (obsd − calcd) from scaled force fields, either B3LYP/cc-pVTZ (dcct) or MP2/cc-pVTZ (mcct). [d] Potential energy distribution (dcct: terms > 5%). [e] Reference 3. [f] Reference 6. [g] Reference 4. [h] Reference 47. [i] Estimated from $\nu_{11} + \nu_{23} = 1336$ cm^{-1} (B_u). [j] From a possible difference band $\nu_{16} - \nu_{13}(B_u)$ observed at 463 cm^{-1} (see text).

belonging to an A″ mode overshadows any A′ type band. No feature near 870 cm^{-1} was reported by Benedetti et al.[45]

2-d$_1$. The feature assigned to ν_9 at 1427 cm^{-1} (liquid) is poorly fitted, and a resonance may be present.

trans-1-d$_1$, *cis-1-d*$_1$. The intrinsically suspect solid-state frequencies for t-1-d_1 are nevertheless quite well reproduced. Seven of the c-1-d_1 A′ modes have not been observed and are represented by dcct predicted values in Table 8.

TABLE 8: Observed Frequencies and Frequency Fit for Five Less Symmetrical Isotopomers of *trans*-1,3-Butadiene in the Region below 2000 cm^{-1}

	c,t-1,4-d_2				2-d_1				*t*-1-d_1				*c*-1-d_1				1,1,2-d_3			
mode[a]	ν_{obsd}[b,c]	ϵ_{dcct}[d]	ϵ_{mcct}[d]	g/u[e]	ν_{obsd}[b,f]	ϵ_{dcct}[d]	ϵ_{mcct}[d]	g/u[e]	ν_{obsd}[b,g]	ϵ_{dcct}[d]	ϵ_{mcct}[d]	g/u[e]	ν_{obsd}[b,g]	ϵ_{dcct}[d]	ϵ_{mcct}	g/u[e]	ν_{obsd}[b,h]	ϵ_{dcct}[d]	ϵ_{mcct}[d]	g/u[e]
A′																				
ν_7	1626 l	−3.1	−3.8	*g*	1635	−1.7	−2.6	g	1645	3.4	2.4	*g*	1630	−11.0	−12.0	*g*	1630	−1.0	−1.7	g
ν_8	1555[i]	−5.0	−5.2	*u*	1587	−7.2	−6.8	u	1580	0.1	0.3	*u*	1571	−7.0	−7.2	*u*	1548.5[j]	2.1	3.0	u
ν_9	1363 l	−3.6	−2.7	*g*	1427 l	−14.1	−12.4	g	1418 s	−3.5	−1.9	*g*	[1426.6]	0.0	1.3	*g*	1425	11.1	12.5	g
ν_{10}	1285	−5.7	−9.8		1380	−1.1	−1.2	u	1304	6.7	4.5	*u*	1346	−0.3	−0.3	*u*	1291.5[j]	0.8	−2.2	u
ν_{11}	1271	−6.7	−3.3	*u*	1292 l	4.1	1.3	g	1288 s	0.1	−3.4	*g*	1291	2.8	0.0	*u*	1185	2.2	0.0	g
ν_{12}	1215 l	−0.2	1.8	*g*	1219 l	1.2	−2.6	g	1270	−4.5	−2.8	*u*	[1225.0]	0.0	2.1	*g*	1075.3[j]	0.2	1.0	
ν_{13}	1146 l	2.1	−2.3	*g*	1073	−0.6	−2.1	u	1185	−2.4	−4.0	*g*	[1163.3]	0.0	−3.1	*g*	1007 s	16.1	14.6	
ν_{14}	[870.5]	0.0	0.6	*u*	890 l	5.5	7.1	g	964 s	9.5	11.1	*u*	[941.0]	0.0	1.0	*u*	880 s	4.8	6.4	
ν_{15}	782 l	1.2	2.5	*g*	878	8.0	11.4	u	793 s	7.8	9.0	*g*	[842.1]	0.0	1.3	*g*	[756.4]	0.0	5.3	
ν_{16}	481 l	1.4	1.7	*u*	508 l	4.2	4.4	g	511 s	5.3	5.4	*g*	[486.3]	0.0	0.1	*g*	484[j] l	8.9	9.5	g
ν_{17}	[275.4]	0.0	0.0	*u*	[292.7]	0.0	−0.2	u	288	1.1	1.1	*u*	[286.0]	0.0	−0.1	*u*	280	8.0	8.0	u
A″																				
ν_{18}	997.4	−0.8	−4.7	*u*	992	−1.5	−4.3	u	1008	−2.6	−7.2	*u*	1009	2.9	0.5	*u*	990.9[j]	−0.3	−3.5	g
ν_{19}	956.5	1.3	0.1	*g*	920 l	5.3	9.4	g	960	3.2	−2.6	*g*	[961.6]	0.0	2.9	*g*	909.2[j]	−2.6	−0.2	g
ν_{20}	850.0	−3.8	3.5	*u*	908	−0.4	−0.1	u	909	−1.7	−0.3	*g*	908	−2.0	−1.1	*u*	791	−1.7	3.7	u
ν_{21}	807.0	3.5	−4.8	*g*	828	2.0	1.5	g	849	−4.6	4.7	*u*	815	4.1	−7.4	*g*	**709.7**[j]	2.4	−3.0	g
ν_{22}	654	−1.1	0.8	*g*	*749* l	−1.6	−3.4	g	674	−17.1	−19.9	*g*	719	−3.0	0.6	*g*	674	−1.2	−2.2	g
ν_{23}	447	1.1	2.1	*u*	498	−2.8	−3.3	u	464	−1.9	−2.7	*u*	491	−2.2	0.9	*u*	439	−0.6	0.3	u
ν_{24}	[156.4]	0.0	0.1	*u*	[158.8]	0.0	0.2	u	[161.1]	0.0	0.4	*u*	[158.0]	0.0	0.0	*u*	[153.0]	0.0	0.1	u

[a] Modes numbered in descending order of frequency as for C_s symmetry. [b] Wavenumber units (cm^{-1}) observed in gas, except where indicated by l (= liquid) or s (= solid). In italics, data employed in the scale factor refinements. Liquid values were so employed only in the A″ species. In brackets, dcct values of unobserved frequencies. In boldface, values differing significantly from previous work. [c] Reference 4, except where otherwise indicated. [d] Frequency fit (obsd − calcd) from scaled force fields, either B3LYP/cc-pVTZ (dcct) or MP2/cc-pVTZ (mcct). [e] Correlation to g or u C_{2h} modes as indicated by the potential energy distribution. No entry signifies no simple discrimination. [f] Reference 48. [g] Reference 46. [h] Reference 46, except where otherwise indicated. [i] Reference 45. [j] Reference 13.

TABLE 9: Scale Factors for Out-of-Plane Bending Force Constants in *trans*-1,3-Butadiene

		sf or Δ_{sf}[b]								
		$w(CH_2)$		$w(CH)$		$\tau(CH_2)$		τ_{skel}		
method[a]		S_{10}, A_u	S_{14}, B_g	S_{11}, A_u	S_{15}, B_g	S_{12}, A_u	S_{16}, B_g	S_{13}, A_u	$F_{11,12}$[c]	ΣWSE[d]
msv	sf	0.9850(63)	0.9730(63)	0.9982(240)	1.0159(104)	0.8975(174)	0.8889(103)	1.0613(100)	0.0144	46.2
mtz	sf	1.0398(77)	1.0289(78)	1.0311(301)	1.0656(129)	0.9154(212)	0.9202(127)	1.1217(128)	0.0150	62.9
mtz+	sf	1.25	1.25	1.05	1.17	0.93	0.99	1.73	0.0155	381.5[e]
mcct	sf	0.9495(35)	0.9531(36)	0.9594(127)	0.9769(58)	0.9114(97)	0.9021(60)	0.9335(50)	0.0144	15.2
mcct	Δ_{sf}	−0.0036(71)		−0.0175(185)		0.0093(157)				
dsv	sf	0.9552(49)	0.9567(52)	0.9568(185)	0.9324(79)	0.9264(146)	0.9186(86)	0.8284(61)	0.0180	29.5
dtz	sf	0.9417(42)	0.9491(45)	0.9494(151)	0.9291(67)	0.9401(123)	0.9281(74)	0.8660(54)	0.0175	21.6
dtz+	sf	0.9370(41)	0.9472(45)	0.9492(148)	0.9301(66)	0.9535(122)	0.9418(74)	0.8776(54)	0.0171	21.0
	Δ_{sf}	−0.0102(86)		0.0191(214)		0.0117(196)				
dtz+*	sf	0.9382(28)	0.9472(31)	0.9248(90)	0.9304(45)	0.9724(78)	0.9432(51)	0.8780(37)	0.0135	11.2
	Δ_{sf}	−0.0090(59)		−0.0056(135)		0.0292(129)				
dcct	sf	0.9254(40)	0.9334(43)	0.9364(142)	0.9153(63)	0.9386(117)	0.9243(71)	0.8558(51)	0.0172	21.6
	Δ_{sf}	−0.0080(83)		0.0211(205)		0.0143(188)				
dcct*	sf	0.9267(29)	0.9333(31)	0.9110(90)	0.9155(45)	0.9581(77)	0.9257(50)	0.8563(36)	0.0135	11.6
	Δ_{sf}	−0.0066(60)		−0.0045(135)		0.0324(127)				
dcct+	sf	0.9217(40)	0.9320(44)	0.9348(142)	0.9146(63)	0.9449(118)	0.9388(72)	0.8616(52)	0.0170	21.9
	Δ_{sf}	−0.0103(84)		0.0202(205)		0.0061(190)				
dcct+*	sf	0.9267(29)	0.9333(31)	0.9110(90)	0.9155(45)	0.9581(77)	0.9257(50)	0.8563(36)	0.0135	12.5
	Δ_{sf}	−0.0066(60)		−0.0045(135)		0.0324(127)				

[a] Key: d = B3LYP, m = MP2; sv = 6-31G*; tz = 6-311G**; tz+ = 6-311++G**; cct = cc-pVTZ; cct+ = aug-cc-pVTZ. * denotes $F_{11,12}$ set to 0.0135 aJ rad^{-2} before scaling. [b] sf = scale factor, with dispersion in parentheses. Δ_{sf} is the $A_u - B_g$ difference, quoted only for the tz+, cct, cct, and cct+ bases. [c] Unscaled value of symmetry force constant in aJ rad^{-2}. [d] Sum of least squares of errors in frequencies for the A″ (= $A_g + B_u$) species. [e] Incomplete convergence after 20 cycles.

1,1,2-d$_3$. Here there are several difficulties. The obs-calc differences of about 12 and 16 cm^{-1} respectively on ν_9 at 1425 and ν_{13} at 1007 cm^{-1} are unacceptably high, even taking into account the fact that the data derive from condensed phase spectra. The same is true for ν_{14} if the liquid-phase value[13] of 890 cm^{-1} is used. Of all the asymmetric isotopomers, 1,1,2-*d*$_3$ should be the one in which the effect of the destruction of the center of symmetry on the forms of the vibrations should be a maximum. Here, if anywhere the effects of constraining equal scale factors for similar motions in the A_g and B_u species should be visible. However, we have left in our refinement only one such constraint and lifting it produced no better fit than that of Table 8. These anomalies therefore remain unexplained. Finally, we consider ν_{15}, expected at 756.4 cm^{-1} (dcct), to be so far unobserved and not to be assigned to the C type band at 733.7 cm^{-1}.[13]

Scaling of the A″ Force Field. For the four A_u and three B_g symmetry coordinates, seven independent scale factors were employed throughout. Results are displayed in Table 9.

We first consider results from the MP2 calculations. An unexpected result was the failure of the MP2/6-311++G** (mtz+) scale factor refinement to converge.[50] This problem originated in the A_u species where a very low value of the diagonal force constant $F_{13,13}$ (skeletal torsion) was associated with a high degree of correlation between the scale factors for S_{11}, S_{12}, and S_{13}. This correlation in itself need not have been a problem in obtaining realistic descriptions of the normal coordinates for the motions, but the enormous value of 382 for ΣWSE, the sum of weighted squares of frequency errors, indicated that there must be major flaws in these normal coordinates. The high values of several of mtz+ scale factors in both A_u and B_g species ($sf_{10} = sf_{14} = 1.25$, $sf_{13} = 1.74$) are associated with low values of the theoretical frequencies of these out-of-plane vibrations, particularly the skeletal torsion. To explore the influence of basis set, calculations were carried out for the bases 6-31G* (sv) and 6-311G** (tz) as well as the correlation consistent set cc-pVTZ. The sv and tz scale factor refinements converged, but the ΣWSE values remained high when compared to their B3LYP counterparts. In stark contrast, the MP2/cc-pVTZ (mcct) refinement was both well behaved and also yielded a ΣWSE value of only 16.5. In addition, the scale factors lay in an acceptable range, 0.91−0.97.

This difference in behavior with the mcct calculation is readily explained by the presence of *f* functions in the cc-pVTZ basis. The necessity of incorporating such *f* functions into the basis for an MP2 calculation, if realistic bending frequencies are to be obtained, has long been recognized in certain types of molecules, namely those involving double and triple bonds.[52−54] Of the latter, C_2H_2, C_2H_4, HCN, CO_2, and the out-of-plane modes of benzene are notable examples. Particular modes, for example the ν_4 B_{2g} vibration of benzene, are affected far more than others in the same molecule.[54] Another feature of these earlier results reflected in our calculations is that the effect of the absence of *f* functions appears to increase markedly with the introduction of polarization and diffuse functions.

As a consequence of this A″ failure of the mtz+ treatment, we abandoned the latter for further calculations such as the harmonic contributions to α constants.

Among the corresponding B3LYP calculations, also shown in Table 9, sf_{13} was only a few percent smaller than the other factors, and there was only a minor effect of basis set. The presence of *f* functions tended to increase the range covered by the factors, causing sf_{13} to fall slightly. While the fit factor ΣWSE was significantly larger with the sv (6-31G*) basis, the dtz+ and dcct calculations gave essentially identical fits. These findings are in line with other B3LYP studies of bending frequencies, which exhibit sensitivity to the presence of *f* functions in C_2H_2 but not in C_2H_4 or C_6H_6.[54] The *f* function effect is therefore modest and variable with a DFT method.

Noticing that a number of frequencies were poorly fitted in each of the B3LYP calculations, the effect was explored of an independent alteration of off-diagonal force constants. In each case a major improvement in the fit resulted when $F_{11,12}$ in the A_u species was reduced to 0.0135 aJ rad^{-2} before scaling. The corresponding treatments are designated in Table 9 by the addition of an asterisk: dtz+*, dcct*, dcct+*. (The value of $F_{11,12}$ in the mcct calculation was already close (0.0144) to the above 0.0135 and was left unchanged.) Subsequent inspection

TABLE 10: Comparison of Observed[a] and Calculated[b] Centrifugal Distortion Constants for Isotopomers of *trans*-1,3-Butadiene

	parent				1-$^{13}C_1$				2,3-$^{13}C_2$			
	obsd	calcd (dcct)[b]	% diff (dcct)[c]	% diff (mcct)[c]	obsd	calcd (dcct)[b]	% diff (dcct)[c]	% diff (mcct)[c]	obsd[d]	calcd (dcct)[b]	% diff (dcct)[c]	%diff (mcct)[c]
Δ_K/kHz	219.4	226.9	3.4	−2.8	217.7	226.7	4.1	−2.2	219	228	3.1	−2.3
Δ_{JK}/kHz	−7.33	−7.32	−0.1	−8.7	−6.93	−7.21	4.0	−4.9	−7.29	−7.40	1.6	−7.0
Δ_J/kHz	0.876	0.889	1.5	2.6	0.812	0.842	3.7	1.1	0.859	0.880	2.4	3.6
δ_J/kHz	0.11	0.11	0	0	0.092	0.102	11	12	0.11	0.11	0	0
δ_K/kHz	4.0	4.0	0	0	4.4	3.8	14	14	3.8	3.9	3	3

	1,1-d_2				2,3-d_2				*t*,*t*-1,4-d_2			
	obsd	calcd (dcct)[b]	% diff (dcct)[c]	% diff (mcct)[c]	obsd	calcd (dcct)[b]	% diff (dcct)[c]	% diff (mcct)[c]	obsd	calcd (dcct)[b]	% diff (dcct)[c]	% diff (mcct)[c]
Δ_K/kHz	136	145	6.6	0.0	98.16	102.94	4.9	−0.7	175	180	2.9	−2.9
Δ_{JK}/kHz	−3.8	−4.05	−7.9	−5.3	−3.05	−3.17	3.9	−8.5	−4.65	−4.69	0.9	−9.0
Δ_J/kHz	0.72	0.72	0	1.4	0.825	0.852	3.3	4.6	0.615	0.630	2.4	3.6
δ_J/kHz	0.089	0.091	2.2	3.4	0.13	0.14	8	8	0.067	0.071	6.0	6.0
δ_K/kHz	3.8	3.5	−8	−8	4.5	3.8	−16	−18	2.8	2.9	4	4

	c,*c*-1,4-d_2				*c*,*t*-1,4-d_2			
	obsd	calcd (dcct)[b]	% diff (dcct)[c]	% diff (mcct)[c]	obsd	calcd (dcct)[b]	% diff (dcct)[c]	% diff (mcct)[c]
Δ_K/kHz	123.7	128.8	4.1	−2.1	156.2	162.5	4.0	−2.0
Δ_{JK}/kHz	−4.79	−4.94	3.1	−6.7	−4.66	−4.90	5.2	−4.9
Δ_J/kHz	0.813	0.828	1.8	3.3	0.704	0.732	3.8	5.1
δ_J/kHz	0.11	0.11	0[e]	9[e]	0.109	0.093	−15	−14
δ_K/kHz	3.9	3.8	−3	−5	[3.0][f]	3.58		

[a] Given to the last decimal place that lacks uncertainty in the fits. Data from refs 2−7. [b] Computed with the scaled B3LYP/cc-pVTZ force field (dcct), rounded to the precision of the observed value. [c] Calcd − obsd as a percentage, for dcct or mcct (MP2/cc-pVTZ) predictions. [d] Based on ref 2 after reassigning the line at 12 914.705 MHz to the transition $38_{4,34} - 37_{5,33}$, omitting the transition at 17 275.345 MHz, and refitting with a full set of quartic centrifugal distortion constants. The uncertainties in the centrifugal distortion constants were much reduced, and the agreement with the calculated values was much improved. [e] This dcct/mcct difference is almost wholly due to rounding error. [f] Estimated from the other two 1,4-d_2 species and used while fitting the remaining rotational constants.

of the harmonic contributions to the alphas indicated that these low lying modes make significant contributions to the α parameters, so that we feel justified in seeking to improve the fit to the observed data in this way. The error vectors for the dcct results for the A″ modes in Tables 7 and 8 are based on this dcct* force field, as are the harmonic corrections to the alphas and centrifugal distortion constants below.

When the scale factors for similar motions in the A_u and B_g symmetry blocks are compared, the only evidence for a need for differing scale factors occurs in the three refinements involving the adjusted $F_{11,12}$ force constant, namely, dtz+*, dcct* and dcct+*. Here, the CH_2 twist scale factors sf_{12} and sf_{16} diverge from each other.

The complete scaled dcct* force field is given in the Supporting Information, Table S4.

A″ Frequency Fit. The relevant data are included in Tables 7 and 8. Only uncertain frequencies will be considered.

2,3-d_2. ν_{15} was reported earlier at 810 cm^{-1} in the liquid Raman spectrum[22] but was omitted in more recent work although a very doubtful feature at 802 cm^{-1} was present.[3] Our calculations place ν_{15} at about 807 cm^{-1}.

trans,trans-1,4-d_2. ν_{16} was not reported in ref 13, but elsewhere a very weak Raman band at 602 cm^{-1} has been observed.[4] The latter agrees poorly with our prediction of 615 cm^{-1} (dcct*).

1,1,4,4-d_4. The value of 608 cm^{-1} for ν_{16} used in our refinement was estimated from the combination band $\nu_{11} + \nu_{16}$ at 1336 cm^{-1} and is excellently fitted.

d_6. ν_{16} has been quoted as lying at 603 cm^{-1}, presumably in a liquid-phase Raman spectrum.[22] No sign of this feature appeared in our own similar spectrum. A weak infrared band was seen at 463 cm^{-1} in the gas phase which could be the difference $\nu_{16} - \nu_{13}$, in which case $\nu_{16} = 605$ cm^{-1}. This value was far enough from our prediction of 596 cm^{-1} to suggest its omission as a datum from the refinement.

trans-1-d_1. Abe[46] assigns a C-type band at 674 cm^{-1} to ν_{22}. Every calculation made by us or in ref 13 placed ν_{22} about 20 cm^{-1} higher. This datum was therefore ignored.

1,1,2-d_3. Here we have used the gas-phase data from Abe except where the accuracy has been improved, as in the cases of ν_{18}, ν_{19}, and ν_{21}.[13] We agree with the latter work in choosing to assign ν_{21} to the C-type band at 709.7 cm^{-1}, rather than the similar band at 734 cm^{-1}, chosen earlier.[46] The excellent fit to 709.7 cm^{-1} leaves little room for the strong Fermi resonance between ν_{21} and $\nu_{17} + \nu_{23}$ postulated by Abe to explain these two C-type bands. A fresh study of a new sample would be useful both here and elsewhere in the spectrum.

^{13}C Shifts. These are included in Table 4. Agreement between observed and calculated shifts (dcct*, mcct) is excellent in cases where resonances are absent and the data are precise. Gas-phase infrared data have the advantage here. In the two instances where the observed shifts are of the wrong sign, extremely weak, broad liquid-phase Raman bands are involved and the predicted shifts are quite small. In assigning observed shifts in the asymmetric isotopomer 1-$^{13}C_1$ for ν_{11} and ν_{15} (C_{2h} numbering system), the lower of two infrared bands here, at 909 and 900 cm^{-1}, is more A_u than B_g in character, so that the shift on ν_{11} from 908.1 cm^{-1}in d_0 is reasonably taken to be 8 cm^{-1}, in agreement with predictions of 7.3 (dcct*) and 7.9 (mcct) cm^{-1}. The broad liquid-phase Raman band at 906 cm^{-1} in the 1-$^{13}C_1$ species is shifted by 2 $cm^{-1}$from the corresponding d_0 liquid band at 908 cm^{-1} and so is better assigned largely to $\nu_{15}(B_g)$, in agreement with predictions of 1.3 (dcct*) and 0.9 (mcct) cm^{-1}. However, it must be borne in mind that the near degeneracy of ν_{11} and ν_{15} in d_0

TABLE 11: Comparison of CH Bond Properties in Ethylene, Propene, and 1,3-Butadiene, from QC Calculations

ν^{is}(CH)/cm^{-1}

		QC method[a]								
		dtz+		dcct		mtz+		mcct		obsd
	bond	ν^{is}(CH)	$\Delta\nu^b$	ν^{is}(CH)	$\Delta\nu^b$	ν^{is}(CH)	$\Delta\nu^b$	ν^{is}(CH)	$\Delta\nu^b$	$\Delta\nu^c$
ethylene		3170.8		3173		3234.5		3237.9		
propene	CH_α	3120.9	−49.9	3123.3	−49.7	3181.2	−53.3	3188.1	−49.8	−40
	CH_c	3156.0	−14.8	3158.3	−14.7	3216.6	−17.9	3220.8	−17.1	−14
	CH_t	3178.7	7.9	3181.3	8.3	3236.9	2.4	3241.9	4.0	11
butadiene	CH_α	3131.6	−39.2	3132.7	−40.3	3182.1	−52.4	3189.9	−48	
	CH_c	3165.0	−5.8	3167.0	−6.0	3219.3	−15.2	3223.8	−14.1	
	CH_t	3190.6	19.8	3192.9	19.9	3242.1	7.6	3247.4	9.5	

Bond Length/Å

		QC method[a]								
		dtz+		dcct		mtz+		mcct		obsd
	bond	r_e(CH)	Δr_e	r_e(CH)	Δr_e	r_e(CH)	Δr_e	r_e(CH)	Δr_e	Δr_e[d]
ethylene		1.085 01		1.082 59		1.085 38		1.080 43		
propene	CH_α	1.088 92	0.0039	1.086 41	0.0038	1.089 69	0.0043	1.084 33	0.0039	
	CH_c	1.086 23	0.0012	1.083 83	0.0012	1.086 94	0.0016	1.081 95	0.0015	
	CH_t	1.084 17	−0.0008	1.081 75	−0.0008	1.085 07	−0.0003	1.080 04	−0.0004	
butadiene	CH_α	1.088 23	0.0032	1.085 90	0.0033	1.089 85	0.0045	1.084 48	0.0041	0.0042
	CH_c	1.085 60	0.0006	1.083 22	0.0006	1.086 87	0.0015	1.081 86	0.0014	0.0014
	CH_t	1.083 33	−0.0017	1.080 92	−0.0017	1.084 75	−0.0006	1.079 71	−0.0007	−0.0012

IR Intensity (A)/km mol^{-1}

		QC method[a]							
		dtz+		dcct		mtz+		mcct	
	bond	A	ΔA	A	ΔA	A	ΔA	A	ΔA
ethylene		10.9		10.7		7.5		6.1	
propene	CH_α	21.1	10.2	20.4	9.7	16.4	8.9	14.1	8.0
	CH_c	12.9	2.0	12.7	2.0	9.1	1.6	7.7	1.6
	CH_t	10.5	−0.4	10.9	0.2	8.0	0.5	6.7	0.6
butadiene	CH_α	13.6	2.7	12.9	2.2	10.8	3.3	8.7	2.6
	CH_c	10.4	−0.5	10.3	−0.4	7.3	−0.2	6.0	−0.1
	CH_t	5.7	−5.2	6.0	−4.7	4.4	−3.1	3.4	−2.7

Mulliken Charge on Hydrogen (q_H)/e

		QC method[a]							
		dtz+		dcct		mtz+		mcct	
	bond	q_H	Δq_H	q_H	Δq_H	q_H	Δq_H	q_H	Δq_H
ethylene		0.1108		0.1155		0.1130		0.1511	
propene	H_α	0.1495	0.0387	0.1121	−0.0034	0.1669	0.0539	0.1562	0.0051
	H_c	0.1125	0.0017	0.1046	−0.0109	0.1253	0.0123	0.1405	−0.0106
	H_t	0.1106	−0.0002	0.1097	−0.0058	0.1132	0.0002	0.1479	−0.0032
butadiene	H_α	0.1245	0.0137	0.1069	−0.0086	0.1487	0.0357	0.1532	0.0021
	H_c	0.1175	0.0067	0.1069	−0.0086	0.1255	0.0125	0.1417	−0.0094
	H_t	0.1333	0.0225	0.1123	−0.0032	0.1439	0.0309	0.1471	−0.0040

[a] Key: dtz+ = B3LYP/6-311++G**, dcct = B3LYP/cc-pVTZ, mtz+ = MP2/6-311++G**, and mcct = MP2/cc-pVTZ. [b] Change from calculated value in ethylene. [c] From ref 55, with a revised value of 3053 cm^{-1} for ν^{is}(CH) in ethylene. [d] From ref 12.

means that the mixing of the A_u and B_g motions in the 1-$^{13}C_1$ isotopomer is likely to be different in the liquid phase from what it is in the gas.

Comparison of Observed and Calculated Centrifugal Distortion Constants. The five quartic centrifugal distortion constants depend only on the A_g quadratic force constants. Table 10 shows a comparison of the observed and calculated centrifugal distortion constants obtained from the scaled B3LYP/cc-pVTZ force field. (The precision quoted for the latter is chosen to match the accuracy of the observed data). Observed-calculated differences are also given for the scaled MP2/cc-pVTZ force field. Overall, the agreement is excellent, bearing in mind that the observed constants are for the ground vibrational state, whereas the calculated ones are for the equilibrium form. Poor agreement between the calculated values and those reported for the 1,1-d_2 species[2] led to a reevaluation of the fit and assignment of the lines for this species. After reassigning one line and rejecting another, as reported in a footnote in Table 10, the satisfactory agreement between observed and calculated values shown in Table 10 was obtained.

Harmonic Contributions to Spectroscopic Alphas. Table S5 in the Supporting Information shows the harmonic contributions to the spectroscopic alphas computed with the scaled dcct*, dtz+*, and mcct force fields, as calculated by the ASYM40 program for use in computing the equilibrium structure for BDE.[12]

Characterization of the CH Bonds. It is useful to relate all the CH bond properties yielded by our QC calculations to those in similar molecules, so that chemical effects of substitution and conformation can be identified and compared.

Table 11 shows the calculated QC values for four such properties in the molecules of ethylene, propene and BDE − *unscaled* isolated CH stretching frequencies ν^{is}(CH) in the appropriate partially deuterated species, bond lengths r_e, infrared intensities for the ν^{is}(CH) transitions and the Mulliken charges on the H atoms concerned. These properties were computed for the various isolated ═CH bonds in ethylene-d_3, propene-d_5, and BDE-d_5. In each case, we display also the changes in these properties from ethylene arising from substitution with the methyl group (propene) or the vinyl group (BDE). The data include the results of B3LYP and MP2 calculations with the 6-311++G** and cc-pVTZ bases. Comparison with experimental values can be made only with $\Delta\nu^{is}$(CH) for propene[55] and with Δr(C−H) for BDE, the latter data from ref 12.

Qualitatively, the effects of the methyl and vinyl substituents are similar from the two QC methods. The CH_α bond is markedly weakened by the adjacent methyl or vinyl group, as has long been known experimentally in the case of propene from both ν^{is}(CH)[55] and local mode studies.[56] The CH_c bond is weakened to a smaller extent in both molecules, while a small concomitant strengthening occurs in the CH_t bond. The choice of basis set, 6-311++G** or cc-pVTZ, has only a modest effect on these changes. However, substantial differences appear when the B3LYP and MP2 results are compared in the case of BDE. The B3LYP calculations give rather less weakening of the CH_α and CH_c bonds but a greater strengthening of the CH_t one, the $\Delta\nu^{is}$(CH) values for the latter being 20 cm^{-1} (B3LYP) and 8−10 cm^{-1} (MP2). As noted earlier, no experimental ν^{is}(CH) values exist with which to evaluate these differences.

The Δr_eCH values follow the above $\Delta\nu^{is}$(CH) changes very closely indeed. Clearly, the B3LYP and MP2 approaches differ somewhat in their assessment of the effects of vinyl substitution, the evidence from the semiexperimental equilibrium structure favoring the latter.

Changes in the infrared intensities ΔA_{CH} involve significant increases for the CH_α bonds in propene and a decrease for the CH_t bond in the case of BDE. Such changes are expected to derive as much from charge flux or flow within the molecule as from static charge.[57]

The Mulliken charges on hydrogen, q_H, in propene and BDE are rather more negative with the cc-pVTZ basis than with 6-311++G**. This produces changes of sign in Δq_H from ethylene to propene or BDE. With the 6-311++G*** basis, Δq_H is similar in both methods for both propene and BDE. With cc-pVTZ, Δq_H values tend to be smaller, with little regularity.

Summary

1. Force fields based on B3LYP and MP2 calculations have been scaled by fitting observed infrared and Raman frequencies, some of these new, from 11 isotopomers of BDE. Among the 18 scale factors so determined, small differences are detected in several cases which involve the same type of motion in differing symmetry classes.

In MP2 force field calculations for the out-of-plane bending modes, the Pople-type basis sets 6-31G*, 6-311G**, and 6-311++G** perform poorly in contrast to the Dunning cc-pVTZ set. This improvement is attributed to the presence of *f* functions in the latter. The theoretical skeletal torsional frequency is particularly sensitive to the absence of *f* functions. B3LYP-based force constants show little such sensitivity. From this point of view, the DFT force fields are preferred.

2. Our scaled force fields have been used to calculate harmonic contributions to vibration−rotation interaction (α) constants and also quartic centrifugal distortion constants. The latter agree well with experimental values measured for the ground vibrational state.

3. In a critical study of both new and old frequency data a number of reassignments and diagnoses of Fermi resonances are made, particularly in the ν(CH) and ν(CD) regions of the spectrum. Prediction of isolated CH stretching frequencies and observation of isolated CD stretching modes together yield results compatible with earlier local mode studies.

4. The three types of CH bond present in *trans*-1,3-butadiene are well characterized by computed differences in length, isolated CH stretching frequency, infrared intensity and Raman activity. Resemblances to similar differences in the three types of C−H bond in propene are quite close.

5. A simplified sample setup for observing Raman spectra of gases is described which has been applied to the d_0, 2,3-d_2, 1,1,4,4-d_4, and d_6 species of BDE.

Acknowledgment. Professor D. W. H. Rankin and Dr S. L. Hinchley are warmly thanked for making available the Edinburgh ab initio facility for running the Gaussian 98 program. The EPSRC National Service for Computational Chemistry Software, (administered by the Department of Chemistry, Imperial College London, South Kensington, London SW7 2AZ) is thanked for the computing time on Columbus. Three Oberlin College students, Scott D. Saylor, Keith A. Hanson, and Michael C. Moore, made major contributions to the synthesis of isotopomers and the recording of spectra. The work at Oberlin was supported by NSF Grant CHE-9710375 and a Senior Scientist Mentor grant from the Dreyfus Foundation. Y.N.P. thanks the N.C.C. for some pleasant days spent at Oberlin College.

Supporting Information Available: Table S1, containing values of scale factors determined for the A′ force field from the frequencies of 6 fully symmetrical and 5 less symmetrical isotopomers, Tables S2 and S3, listing the unscaled infrared intensities and Raman activities for the above isotopomers, respectively, Table S4, showing the scaled dcct+ force field, Table S5, consisting of the harmonic contributions to the α constants from the scaled dtz+*, dcct*, and mcct force fields, and Figures S1−S4, showing the gas-phase Raman spectra of the d_0, 2,3-d_2, 1,1,4,4-d_4, and d_6 species, respectively. This material is available free of charge via the Internet at http://pubs.acs.org.

References and Notes

(1) Kveseth, K.; Seip, R.; Kohl, D. *Acta Chem. Scand. A* **1980**, *34*, 31 and references therein.

(2) Caminati, W.; Grassi, G.; Bauder, A. *Chem. Phys. Lett.* **1988**, *148*, 13.

(3) Craig, N. C.; Davis, J. L.; Hanson, K. A.; Moore, M. C.; Weidenbaum, K. J.; Lock, M. *J. Mol. Struct.* **2004**, *695*−*696*, 59.

(4) Craig, N. C.; Hanson, K. A.; Pierce, R. A.; Saylor, S. D.; Sams, R. L. *J. Mol. Spectrosc.* **2004**, *228*, 401.

(5) Craig, N. C.; Hanson, K. A.; Moore, M. C.; Sams, R. L. *J. Mol. Struct.* **2005**, *742*, 21.

(6) Craig, N. C.; Moore, M. C.; Patchen, A. K.; Sams, R. L. *J. Mol. Spectrosc.* in press.

(7) Botschwina, P. *J. Mol. Phys.* **2005**, *103*, 1441.

(8) Groner, P.; Warren, R. D. *J. Mol. Struct.* **2001**, *599*, 323.

(9) Matzger, A. J.; Lewis, K. D.; Nathan, C. E.; Peebles, S. A.; Peebles, R. A.; Kuczkowski, R. L.; Stanton, J. F.; Oh, J. J. *J. Phys. Chem. A* **2002**, *106*, 12110.

(10) Demaison, J.; Møllendal, H.; Perrin, A.; Orphal, J.; Kwabia Tschana, F.; Rudolph, H. D.; Willaert, F. *J. Mol. Spectrosc.* **2005**, *232*, 174.

(11) Craig, N. C.; Groner, P.; McKean, D. C.; Tubergen, M. J. *Int. J. Quantum Chem.* **2003**, *95*, 837.

(12) Craig, N. C.; McKean, D. C.; Groner, P. *J. Phys. Chem. A* **2006**, *110*, 7461.

(13) Panchenko, Yu. N.; Vander Auwera, J.; Moussaoui, Y.; De Maré, G. R. *Struct. Chem.* **2003**, *14*, 337.
(14) Craig, N. C.; Petersen, K. L.; McKean, D. C. *J. Phys. Chem. A* **2002**, *106*, 6358.
(15) McKean, D. C. *Chem. Soc. Rev.* **1978**, *7*, 399.
(16) For example: Bock, C. W.; George, P.; Trachman, M. *Theor. Chim. Acta* **1984**, *64*, 293. Bock, C. W.; Panchenko, Yu. N.; Krasnoshchiokov, S. V.; Pupyshev, V. I. *J. Mol. Struct.* **1985**, *129*, 57. Guo, H.; Karplus, M. *J. Chem. Phys.* **1991**, *94*, 3679. Lee, J. Y.; Hahn, O.; Lee, S. J.; Choi, H. S.; Shim, H.; Mhin, B. J.; Kim, K. S. *J. Phys. Chem.* **1995**, *99*, 1913. Craig, N. C.; Oertel, C. M.; Oertel, D. C.; Tubergen, M. J.; Lavrich, R. J.; Chaka, A. M. *J. Phys. Chem. A* **2002**, *106*, 4230.
(17) McKean, D. C. *J. Mol. Struct.* **1984**, *113*, 251.
(18) Demaison, D.; Wlodarczak, G. *Struct. Chem.* **1994**, *5*, 57.
(19) Swanton, D. J.; Henry, B. R. *J. Chem. Phys.* **1987**, *86*, 4801.
(20) Kjaergaard, H. G.; Turnbull, D. M.; Henry, B. R. *J. Chem. Phys.* **1993**, *99*, 9438.
(21) Duncan, J. L. *Spectrochim. Acta* **1991**, *47A*, 1.
(22) Wiberg, K. B.; Rosenberg, R. E. *J. Am. Chem. Soc.* **1990**, *112*, 1509.
(23) Rosenberg, R. E. Ph.D. Thesis, Yale University, 1988.
(24) Frisch, M. J.; Trucks, G. W.; Schlegel, H. B.; Scuseria, G. E.; Robb, M. A.; Cheeseman, J. R.; Montgomery, J. A., Jr.; Vrevin, T.; Kudin, K. N.; Burant, J. C.; Millam, J. M.; Iyengar, S. S.; Tomasi, J.; Barone, V.; Mennucci, B.; Cossi, M.; Scalmani, G.; Rega, N.; Petersson, G. A.; Nakatsuji, H.; Hada, M.; Ehara, M.; Toyota, K.; Fukuda, R.; Hasegawa, J.; Ishida, M.; Nakajima, T.; Honda, Y.; Kitao, O.; Nakai, H.; Klene, M.; Li, X.; Knox, J. E.; Hratchian, H. P.; Cross, J. B.; Stratmann, R. E.; Burant, J. C.; Dapprich, S.; Millam, J. M.; Daniels, A. D.; Kudin, K. N.; Strain, M. C.; Farkas, O.; Tomasi, J.; Barone, V.; Cossi, M.; Cammi, R.; Mennucci, B.; Pomelli, C.; Adamo, C.; Jaramillo, J.; Goperts, R.; Adamo, C.; Clifford, S.; Ochterski, J.; Petersson, G. A.; Ayala, P. Y.; Cui, Q.; Morokuma, K.; Malick, D. K.; Rabuck, A. D.; Raghavachari, K.; Foresman, J. B.; Cioslowski, J.; Ortiz, J. V.; Baboul, A. G.; Stefanov, B. B.; Liu, G.; Liashenko, A.; Piskorz, P.; Komaromi, I.; Gomperts, R.; Martin, R. L.; Fox, D. J.; Keith, T.; Al-Laham, M. A.; Peng, C. Y.; Nanayakkara, A.; Gonzalez, C.; Challacombe, M.; Gill, P. M. W.; Johnson, B.; Chen, W.; Wong, M. W.; Andres, J. L.; Gonzalez, C.; Head-Gordon, M.; Replogle, E. S.; Pople, J. A. Gaussian 03, Revision B.05, Gaussian Inc.: Pittsburgh PA, 2003.
(25) Dunning, T. H. *J. Chem. Phys.* **1989**, *90*, 1007.
(26) Woon, D. F.; Dunning, T. H. *J. Chem. Phys.* **1993**, *98*, 1358.
(27) Hedberg, L.; Mills, I. M. *J. Mol. Spectrosc.* **2000**, *203*, 82.
(28) An injudicious increase in the number of scale factors, undertaken to explain all the experimental data, runs the risk of a failure to identify the occasional experimental datum which is in error, for instance a frequency which is subject to an overlooked Fermi resonance, or has been simply misassigned.[29−31]
(29) Panchenko, Yu. N. *J. Mol. Struct.* **2001**, *567−568*, 217.
(30) Panchenko,Yu. N.; De Maré, G. R. *J. Mol. Struct.* **2002**, *611*, 147.
(31) Panchenko,Yu. N.; Bock, C. W.; De Maré, G. R. *J. Struct. Chem.* **2005**, *46*, 53.
(32) Choi, C. H.; Kertesz, M.; Dobrin, S.; Michl, J. *Theor. Chem. Acc.* **1999**, *102*, 196.
(33) In the case of the ν(C═C) scale factors, which are essentially determined by the infrared and Raman frequencies in the 1500−1700 cm^{-1} region, the experimental data would need to be similarly influenced by anharmonicity or by Fermi resonance for a difference in scale factor to be significant.
(34) Pulay, P.; Fogarasi, G.; Pongor, G.; Boggs, J. E.; Vargha, A. *J. Am. Chem. Soc.* **1983**, *105*, 7073.
(35) Pupyshev, V. I.; Panchenko, Yu. N.; Bock, C. W.; Pongor, G. *J. Chem. Phys.* **1991**, *94*, 1247.
(36) See, for example: McKean, D. C. *J. Mol. Struct.* **2002**, *642*, 25. Murphy, W. F.; Zerbetto, F.; Duncan, J. L.; McKean, D. C. *J. Phys. Chem.* **1993**, *97*, 581.
(37) McKean, D. C. *J. Phys. Chem. A* **2003**, *107*, 6538.
(38) McKean, D. C. *Spectrochim. Acta* **1992**, *48A*, 1335.
(39) McKean, D. C. *Spectrochim. Acta* **1973**, *29A*, 1559.
(40) The theory is further discussed in: Panchenko, Yu. N.; Pupyshev, V. I.; Bock, C. W. *J. Mol. Struct.* **2000**, *550−551*, 495.
(41) The presence of significant coupling between ν(C═C) and ν(CD) motions in certain cases may of course entail the use in ethylenes[42] of a factor slightly different in value from that of 1.011, which has been found appropriate in saturated compounds.[36] However, there is no evidence for appreciable ν(C═C) motion in the ν^{is}(CD) normal coordinates here.
(42) Duncan, J. L.; Ferguson, A. M. *J. Chem. Phys.* **1988**, *89*, 4216.
(43) Halonen, M.; Halonen, L.; Nesbitt, D. J. *J. Phys. Chem. A* **2004**, *108*, 3367.
(44) Huber-Wälchi, P.; Günthard, Hs. H. *Spectrochim. Acta* **1981**, *37A*, 285.
(45) Benedetti, E.; Aglietto, M.; Pucci, S.; Panchenko, Yu. N.; Pentin, Yu. N.; Nikitin, O. T.*J. Mol. Struct.* **1978**, *49*, 293.
(46) Abe, K. Ph.D. Thesis, Tokyo University, Tokyo, Japan, 1970.
(47) Cole, A. R. H.; Green, A. A.; Osborne, G. A. *J. Mol. Spectrosc.* **1973**, *48*, 212.
(48) Borshagovskaya, L. S.; Panchenko, Yu. N.; Pentin, Yu. N. *Opt. Spectrosc.* **1967**, *22*, 194.
(49) Panchenko, Yu. N.; Pentin, Yu. A.; Tyulin, V. I.; Tatevskii, V. M. *Opt. Spectrosc.* **1962**, *13*, 488.
(50) Incomplete convergence is obviously connected with an ill-conditioned equation system used for the determination of the scale factors.[51.]
(51) Panchenko, Yu. N.; Abramenkov, A. V. *Russ. J. Phys. Chem.* **2003**, *77*, 956.
(52) Simandiras, E. D.; Rice, J. E.; Lee, T. J.; Amos, R. D.; Handy, N. C. *J. Chem. Phys.* **1988**, *88*, 3187.
(53) Simandiras, E. D.; Handy, N. C.; Amos, R. D. *J. Phys. Chem.* **1988**, *92*, 1739.
(54) Handy, N. C.; Maslen, P. E.; Amos, R. D.; Andrews, J. S.; Murray, C. W.; Laming, G. J. *Chem. Phys. Lett.* **1992**, *197*, 506.
(55) McKean, D. C. *Spectrochim. Acta* **1975**, *31A*, 861.
(56) Wong, J. S.; Moore, C. B. *J. Chem. Phys.* **1982**, *77*, 603.
(57) Gussoni, M.; Jona, P.; Zerbi, G. *J. Chem. Phys.* **1983**, *78*, 6802.